ALTERNATE FUELS FOR ON-ROAD ENGINES AND IMPACT ON REDUCING CARBON FOOTPRINT

by

Vrushali Deshmukh

A Thesis

Submitted to the Faculty of Purdue University

In Partial Fulfillment of the Requirements for the degree of

Master of Science in Mechanical Engineering

School of Mechanical Engineering

West Lafayette, Indiana

August 2021

THE PURDUE UNIVERSITY GRADUATE SCHOOL
STATEMENT OF COMMITTEE APPROVAL

Dr. Gregory M Shaver, Chair
School of Mechanical Engineering

Dr. Peter H Meckl
School of Mechanical Engineering

Dr. John T Evans
School of Agricultural and Biological Engineering

Approved by:
Dr. Nicole L. Key

To God and my parents

ACKNOWLEDGMENTS

To begin with, I would like to express my deepest gratitude and appreciation to my advisor, Dr. Greg Shaver, who gave me an opportunity to work on exciting projects and provided guidance, encouragement and support all throughout my journey at Purdue. I feel extreme gratitude for him and feel proud to be associated with Shaver research group.

I would also like to thank my colleagues at Herrick Labs. Miles Droege for his incredible help and vast knowledge in test cell work, Chisom Emegoakor, Shubham Agnihotri and Doni Thomas with whom I have been fortunate to work, special mention to our 'journal club' meetings and subsequent discussions. A shout out to Ryan Thayer for being a go-to person for anything and everything related to test cell. Our project manager Dr. Eric Holloway for making sure we never lost track and any issues were timely addressed. I would also like to thank my lab-mates, including Brady Black, John Foster and Shubham Ashta for their timely support and suggestions. I would also like to extend a big thank you to our project sponsors at Cummins and National Biodiesel Board including Lisa Farrell, Akash Desai, Scott Fenwick and Steve Howell.

Last, but not the least I would like to thank my friends and family. My father for instilling the vision in me for higher education, my mother for being my first guru, my brother Vaibhav whose constant encouragement and support kept me going, my friends Harsha Rao for proofreading the first draft, Shubham Dubey, Kush Paliwal and Rujuta Barve for being my family away from family.

TABLE OF CONTENTS

LIST OF TABLES

LIST OF FIGURES

ABBREVIATIONS

AFR	Air-Fuel Ratio
ASC	Ammonia Slip Catalyst
BSFC	Brake Specific Fuel Consumption
BTE	Brake Thermal Efficiency
CCE	Closed Cycle efficiency
CDA	Cylinder de-activation
CG	Center of Gravity
COMF	Combustible Oxygen Mass Fraction
DOC	Diesel Oxidation catalyst
DOE	Design of Experiments
DPF	Diesel Particulate Filter
ECM	Engine Control Module
ECR	Effective Compression Ratio
EGR	Exhaust Gas Recirculation
EIA	Energy Information Administration
EPA	Environmental Protection Agency
ft	Foot
FMEP	Friction Mean Effective Pressure
IV	Intake Valve
EIVC	Early Intake Valve Closure
IC	Internal Combustion
IVC	Intake Valve Closure
LIVC	Late Intake Valve Closure
HD-FTP	Heavy Duty Federal Test Procedure
lbs.	Pounds
MY	Marketing Year
NBB	National Biodiesel Board
NSB	National Soybean Board
NOx	Oxides of Nitrogen

NVH	Noise Vibration Harshness
OCE	Open Cycle Efficiency
ppm	Parts per million
PM	Particulate Matter
PMEP	Pumping Mean Effective Pressure
RFS	Renewable Fuel Standard
RPM	Revolutions Per Minute
SCR	Selective Catalytic Reduction
UBHC	Un -Burnt Hydrocarbon
ULSD	Ultra-Low Sulfur Diesel
VVA	Variable Valve Actuation

ABSTRACT

Variable valve actuation remains one of the most studied technologies for diesel engines for fuel benefits, efficiency improvements and emission control. The same can be implemented on natural gas engines however presence of throttle valve in the spark ignited natural gas engine leads to different set of challenges and outcomes. In this document, focus is on GT power led analyses for a mid-range natural gas engine and the VVA strategy applied is modulation of intake valve closure timing. The simulations are run for early intake valve closure and late intake valve closure, both applied independently and run for steady state conditions. The focus is on the low torque range to study the impact of IVC modulation on throttling losses for low torque region. The simulation studies showed that IVC strategies both early as well as late IVC do benefit in terms of thermal efficiency improvements by up to 3% and reduction in brake specific fuel efficiency by up to 13%. It also showed considerable reduction in pumping loop and increase in open cycle efficiency when IVC modulation is applied. Validating the model further with real on-engine data and then calibrating the existing GT power with the on-engine data to validate the conclusions drawn would be the next set of goals for this project.

Second part of this document is focused on real life testing of soy biodiesel fueled heavy duty on-road engine with modern exhaust aftertreatment system with SCR. Soybean based biodiesel remains one of the most sought-after alternate fuel and biofuel to be used in on-road engines. Burning biodiesel leads to a cleaner exhaust compared to conventional diesel as the biofuel is oxygenated fuel leading to more complete combustion and lower amount of emission species such as CO, CO_2 and PM in the exhaust. The experiments discussed in this document consisted of developing torque curve envelopes and steady state tests (RMC set points). Three soy biodiesel blends were studied which included B20- 20% biodiesel, B50 – 50% biodiesel and B100 – 100% biodiesel. NOx emissions were observed to be considerably higher for B100 at engine outlet by up to 80% as well as at tailpipe outlet increased by up to 380 %, compared to that of conventional diesel which is attributed to the thermal mechanism of NO production. The exhaust gas temperatures were observed to be lower by up to 40-degree C while the urea dosing was considerably higher by up to 83 % when using biodiesel blend B100. This research paves the way to testing further using varying biodiesel blends for regulation certification trials, for tuning the

diesel engines for different biodiesel blends and for developing the control strategy for the existing diesel engines to accommodate biodiesel.

1. INTRODUCTION

1.1 Role of alternate fuels

As the world continues to take steps towards being carbon-neutral, the automotive industry worldwide has been working on taking measures towards it as well. Working on options for alternate fuels as an alternative to gasoline and diesel has been a continuous effort. Alternate fuels, also referred to as non-conventional fuels, are any materials which can be used as fuel in place of conventional fuels. Some of the examples include hydrogen, natural gas, electricity, alcohol-based fuels like ethanol, butanol and vegetable-based oils such as soybean oil, sunflower oil, canola oil and so on.

The emission norms are becoming stringent worldwide and in the United States of America. The U.S. Environmental protection agency (EPA) is requiring major reduction in sulfur content of diesel fuels. Ultra-low sulfur diesel (ULSD) is a cleaner diesel fuel with a maximum 15 parts-per-million (ppm) sulfur. Most of the diesel fuel now sold in the United States for use in vehicles is ULSD fuel [1].

As per the EPA emissions regulations for on-highway diesel engines from model year 2007 onwards, the engines are required to operate with only the ultra-low sulfur diesel (ULSD).
The low sulfur fuel prevents fouling of the after-treatment systems and thus aids in reducing the emissions. Also, objective of using ULSD fuel coupled with advanced exhaust emission control systems is to reduce the particulate matter emissions by up to 90% and emissions of nitrogen compounds (NOx) by 25% to 50%. ULSD fuel helps reduce emissions in older engines as well [1].

The shift from the existing diesel engine vehicles to the advanced cleaner diesel engine vehicles will take a while, thus the existing diesel engine vehicles still make a significant contribution to air pollution.

According to the estimate by the U.S. Energy Information Administration (EIA), diesel fuel consumption in the U.S. transportation sector in 2019 resulted in the emission of 456 million metric tons of carbon dioxide (CO_2), a greenhouse gas. This amount was equal to about 24% of total U.S. transportation sector CO_2 emissions and equal to approximately 9% of total U.S. energy-related CO_2 emissions in 2019 [2]. These numbers further reiterate the need to work on cleaner alternate fuel options for diesel.

Natural gas makes an attractive option from the available alternate fuels, as it is an efficient, relatively clean burning fuel as well as economical energy source.

Natural gas is a clean burning fossil fuel relative to diesel. The use of natural gas as fuel results in much less emissions of all types and especially CO_2 compared to using coal or diesel when compared to production of the same amount of energy. About 117 pounds of carbon dioxide is produced per million British thermal units (MMBtu) equivalent of natural gas as compared to more than 200 pounds of CO_2 per MMBtu of coal and more than 160 pounds per MMBtu of distillate fuel oil [2]. This has increased the use of natural gas for electricity generation as well as for fuel for on-road vehicles in the United States.

One of the major issues with natural gas is that it is mainly composed of methane which is a strong greenhouse gas. Also, leakage of natural gas into the atmosphere from oil and natural gas wells, storage tanks, pipelines, and processing plants pose another set of challenges. The U.S. Environmental Protection Agency estimates that in 2018, methane emissions from natural gas and petroleum systems and from abandoned oil and natural gas wells were the source of about 29% of total U.S. methane emissions and about 3% of total U.S. greenhouse gas emissions [2]. It is required that the oil and natural gas industry take steps to prevent natural gas leaks. Natural gas exploration, drilling, and production affects the environment. The exploration efforts to locate the source of natural gas deposits lead to leveling an area around the site as well as disturbing the plants and vegetation around the site. Another issue with the natural gas extraction efforts is that natural gas wells and pipelines often have engines to run equipment and compressors, which produce air pollutants and noise, which is another source of pollution [2] .

The second alternate fuel of interest in this document is biodiesel. While natural gas has some advantages and some challenges in terms of its production, biodiesel use in diesel engines does not have similar negative effects. Use of soybean oil for biodiesel was greatly influenced by promotion from U.S. soybean farmers through the United Soybean Board (USB) and subsequent creation of the National Biodiesel Board (NBB) [3].

While biodiesel can be produced from a variety of sources, use of soybean-based biodiesel has an increasing share in it, especially in the United States, currently at 30% of domestic soybean oil disposition. It is the most used oil for biodiesel production and during marketing year (MY), which ran from October 1, 2017, to September 30, 201, inputs reached 7.1 billion pounds. Federal biodiesel mandates only encouraged the further production of biodiesel for a large part of soybean

oil to be used for biodiesel production. The figure below shows increasing amount of use of soybean oil as biodiesel between MY 2012 to MY 2018 [4].

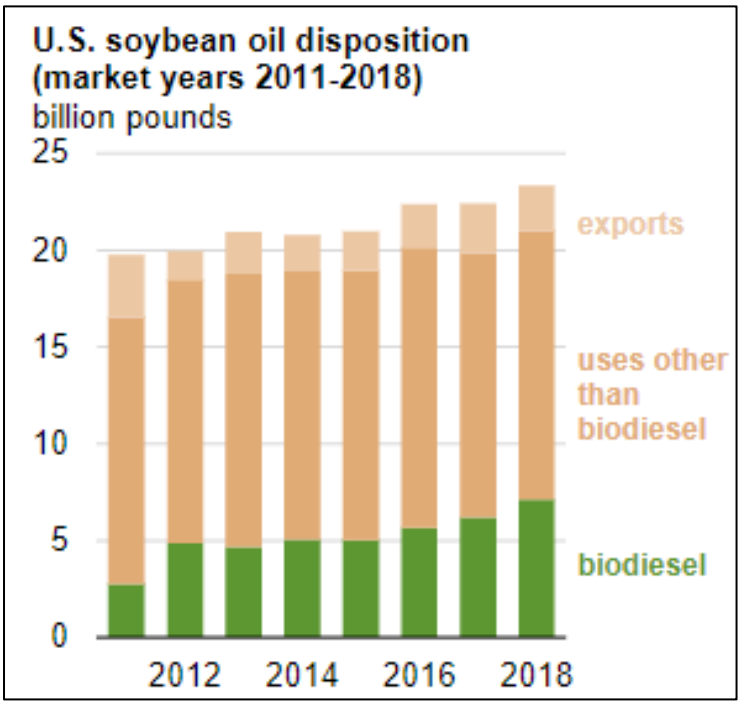

Figure 1: U.S. Soybean oil disposition 2011-2018 [5]

Chemically, biodiesel is an ester, a mix of alkyl esters to be specific and it can be produced from different sources like vegetable oils, fats, plants and so on. In total, vegetable oils comprise about three-fourths of total biodiesel feedstock in the United States, wherein soybean oil share is slightly more than half of total inputs by weight. Smaller amounts of vegetable oil for biodiesel production include distiller's corn oil (an inedible oil that is produced as a byproduct of the corn ethanol production process) and canola oil. Soybean oil and distiller's corn oil are widely used because the feedstocks are produced in the Midwest region of the United States, where most biofuel production capacity exists.

About half of U.S. raw soybeans are exported, and the remaining are processed, or crushed at soybean processing plants in the United States. The soybean crush yields about 80% soybean meal and 20% soybean oil, which may be further processed into various food and non-food products [4].

As total U.S. soybean oil supply grew between MY 2010–2011 and MY 2017–2018, from about 22.5 billion pounds to nearly 26.0 billion pounds, the share of total soybean oil consumed

as a biodiesel feedstock doubled, from about 15% to 30% [4]. Soybean oil and other vegetable oils may also be used as a feedstock for renewable diesel, a separate biofuel that is increasingly produced at stand-alone facilities and petroleum refineries.

As seen in fig 1, biodiesel production increased from 0.7 billion gallons to 1.8 billion gallons between MY 2010–2011 and MY 2017–2018. This could be credited to the mandate of Environmental Protection Agency of blending renewable fuel with nation's fuel supply via Renewable Fuel Standard (RFS), a program administered by the U.S. EPA. As a result, the target for biofuel went to 2.10 billion gallons from 1.15 billion gallons from year 2010 to year 2018 [4]. Finally, there are a few challenges with biodiesel production and use. First one is production challenges related to cost and profitability. Second is the issue of insects and pests for the soybean crops and lead to challenges relating to crops harvest. And lastly, another challenge is soybean oil gets frozen at sub-zero temperatures and thus require making sure the use of anti-freeze agents in the soy biodiesel or heated fuel lines or some similar arrangements during winter season.

1.2 Outline

This thesis document comprises of two distinct studies involving two different alternate fuels and different sets of experiments. Both studies, however, centered on cleaner emissions. First are variable valve actuation strategies for a natural gas engine where GT power-based simulations are run to study the effects of intake valve closure modulations on brake thermal efficiency and fuel consumption. Second study is an experimental study of effect of using soy biodiesel on a heavy duty on highway engine in steady state conditions and NOx emissions there upon.

Variable valve actuation refers to varying the valve timings for the internal combustion engine. Advancing and/or delaying the opening and closing of intake and exhaust valves have proven beneficial for diesel engines in terms of reduction in NOx and unburnt hydrocarbons (UBHC) [6]. However, in case of spark ignited engines like gasoline fueled and natural gas fueled engines, one of the main concerns is throttling losses at low torque conditions. Another performance limitation for an SI engine is knock tendency of the engine. Knock is auto-ignition of fuel before getting ignited by the flame and it creates a shock wave surging in-cylinder pressure beyond the design limits.

The analyses run here were solely focused on studying the effect of IVC modulation on pumping losses at low load conditions. Subsequent sections (section 2, 3 and 6) discuss the model setup in detail, inputs applied, the issues faced during simulations and results and conclusions.

In the biodiesel study, soy biodiesel blends of varying compositions were studied in steady state conditions. A total of 3 blends, B20, B50 and B100 were chosen for the experimentation purpose. Since biodiesel is oxygenated fuel, it contains about 10-15% oxygen by mass. Due to this, there will be complete combustion of hydrocarbons leading to lesser CO, CO_2 and PM while it also leads to NOx production by thermal mechanism. Biodiesel also has a higher cetane number compared to conventional diesel. The higher the cetane the number, the shorter the ignition delay is, thus there will be a longer residence time for combustion products inside the cylinder. And longer residence times at higher temperatures increase thermal NOx production, wherein higher temperatures than adiabatic flame temperatures are attributed to complete combustion due to oxygen bound fuel – biodiesel.

The mechanism explaining thermal NOx production is known as Zeldovich phenomenon. Following are the reactions involved in Zeldovich phenomenon

$$N_2 + O \leftrightarrow NO + N - (1)$$

$$N + O_2 \leftrightarrow NO + O - (2)$$

The overall global reaction is given as –

$$N_2 + O_2 \leftrightarrow 2NO - (3)$$

The fuel properties of diesel and B100 are as below –

Table 1: Fuel properties

Property	Diesel	B100
Density	828 g/L	863 g/L
HHV	49.65	41.33 MJ/Kg
Flash point	321 K	439 K
Viscosity	2.76 cSt	4.16 cSt
Cetane number	42-45	45-60

With reference to table 1, biodiesel has higher fuel density, lower heating value, higher flash point, higher viscosity and higher cetane number as compared to conventional diesel.

Experimental setup, results and conclusions drawn thereon are discussed in sections 4, 5 and 6 of this document.

1.3 Literature review

Natural gas VVA

R Modiyani and L Kocher et. al performed a study about impact of IVC modulation on effective compressions ratio. The study focused on determining the changes needed in control strategies based on ECR when IVC is applied on diesel engines and on developing control strategies. Simulation based steady state analyses were run to study the effects of IVC timing, EGR flow and variable geometry turbine on ECR, charge flow and EGR fraction. ECR was calculated as below

$$ECR = \frac{Effective\ Volume\ at\ IVC}{Effective\ Volume\ at\ TDC}$$

It was concluded that with IVC modulation whether advancing and delaying, affected the ECR the most. ECR reduced with IVC modulation with charge flow into the cylinder being reduced and it also directly affected volumetric efficiency. However, it was established that the trade-off between ECR and volumetric efficiency could be solved by optimizing the IVC modulation [7].

Akash Garg and Mark Magee et.al studied the effects of cylinder throttling via intake valve closure modulations on thermal management of after treatment systems. Additionally, this study also focused on effects of IVC modulation on emissions, fuel consumption and in-cylinder combustion. They highlighted that IVC modulations result in reducing the volumetric efficiency which further results in increase in exhaust gas temperatures. The experimental studies proved that both late as well as early in take valve closures yielded similar effect [8].

The study also indicated that while there was no significant change in mechanical and closed cycle efficiency, brake thermal efficiency increases. This was because, the pumping loops are reduced with early and late IVC timings results, and lead to lower pumping mean effective pressures (PMEPs) which led to higher open cycle efficiency. Improvements were observed on emissions as well, BS NOX reduced, and so were PM emissions.

Kuruppu, C., Pesiridis, A., and Rajoo, S., studied the effect of combined strategy of CDA and VVA on a gasoline fueled engine. CDA has known issues related to NVH which restrict the

use of CDA. Simulation studies performed for CDA alone and for CDA in combination with VVA showed improvements in BSFC and reduction in PMEP at part loads for the combination strategy as compared with only CDA[9].

Biodiesel work

Study performed by Gayatri Adi et.al pointed out that there was substantial increase in NOx as compared to conventional diesel. This study indicated that, when using biodiesel, torque was reduced up to 12%; NOx increased by up to 38% and fuel consumption increased by up to 13%. The study hypothesized the reasons behind above observations as autoignition characteristics, PM-NOx relation, bulk modulus and adiabatic flame temperature. Although the paper points out that there was no certainty about adiabatic flame temperature, whether it is lower or higher for biodiesel. The autoignition characteristics were attributed to the high cetane number of biodiesel which led to quick ignition thus resulting in reduced mixing, longer residence times and increased temperatures which led to increase in NOx. The PM-NOx relation refers to the point that since biodiesel produces lower PM, it results to less radiant heat loss and higher temperatures resulting in more NOx. The bulk modulus hypothesis referred to the point that biodiesel travels faster through fuel lines due to increased speed of sound in biodiesel resulting in increase in injection timings. Advanced injection further leads to more residence times and higher peak temperatures due to more heat release at TDC.

David Snyder et.al performed a study to approach closed loop control for accommodating biodiesel blends based on combustible oxygen mass fraction (COMF) and injected fuel energy. It was also suggested to modify the control strategy to replace EGR fraction by COMF and replace fuel injection by mass with fuel injection by energy. The experimental validation for modified control strategy showed torque for B100 (100% biodiesel) at par with diesel and reduced NOx, lower PM, combustion noise and improved efficiency [10].

The study performed by Carry Hall et.al further delved into verifying the effectiveness of the control algorithms developed based on COMF and energy-based fuel injection on fatty acid contents in biodiesel. They did experimental validation for two soybean-based biodiesel blends with different fatty acid compositions. Their study showed that biodiesel with varying fatty acid structures have very similar fuel energy content as well as heat release rates hence the energy-based controller could be applied to any biodiesel blend of varying fatty acid composition. Their

study further iterated that since during mixing controlled combustion, diesel and biodiesel have very similar injection timing and rate of combustion, biodiesel torque can be matched to that of diesel, by increasing the fuel quantity to match the fuel energy [11].

A textbook on 'Biodiesel Combustion performance and emission characteristics', by Semkula Maroa and Freddie Inambao further deep dives in the subject. The book starts with discussion on NOx formation routes in the internal combustion engines. The main source of Nitrogen in IC engines being atmospheric Nitrogen (N_2). The book further documents five main NOx formation mechanisms that are: Zeldovich (thermal NOx), Fenimore (prompt Nox), N_2O (nitrous oxide), fuel-bound (fuel-bound nitrogen), and diazanul (NNH) [12].

Zeldovich and Fenimore (thermal and prompt) mechanisms are considered the dominant mechanisms.

Zeldovich Route (Thermal NOx) occurs at temperatures above 1700 K and includes following reactions as previously stated, in equations 1 and 2.

$$N_2 + O \leftrightarrow NO + N - (4)$$

$$N + O_2 \leftrightarrow NO + O - (5)$$

$$N + OH \leftrightarrow NO + H - (6)$$

The Zeldovich mechanism takes the intermediate route especially in lean fuel ($\theta < 0.8$)

$$O + N_2 + M \leftrightarrow N_2O + M - (7)$$

$$H + N_2O \leftrightarrow NO + NH - (8)$$

$$O + N_2 \leftrightarrow NO + NO - (9)$$

Factors that affect the Zeldovich Mechanism mainly are residence time in the combustion chamber and concentration of N_2 and O_2 in the combustion chamber [12].

Fenimore Route (Prompt NOx) is when the stoichiometric ratio is higher, it leads to formation of higher NOx.

The book further discussed factors affecting production of NOx when using biodiesel. The cause of high NOx emissions in biodiesel is conflicting and disputed in research circles Some link it to the physiochemical properties of biodiesel. Some link it to the high oxygen content (which leads to incomplete combustion, reduced UHC, reduced CO, and increased combustion temperatures). Some also suggest the high bulk modulus leads to increased fuel injection and longer residence times. Some studies link it to the adiabatic flame temperature (but contradicting evidence has been shown for lower and higher flame temperatures compared to

diesel) while some link it to the heat release (but again contradicting evidence suggests the biodiesel causes the heat release to increase/decrease) [12].

It was also discussed that increased ignition delay has been linked to increased pre-mixed burnt fraction which is a predominant factor in NOx formation. Some studies link it to the Sauter mean diameter.

The oxygen content of the biodiesel reduces the quantity of the air that the injected fuel mixed with before combustion. The lower mixing means larger quantities of fuel are injected. Effect of adiabatic flame temperature from unsaturated molecules is higher compared to saturated molecules.

It was also reported that biodiesel fuels have been observed to give higher adiabatic flame temperatures compared to diesel due to their high concentration of unsaturated molecule structures. Studies have also found lower adiabatic flame temperatures for biodiesel. Because of the high oxygen content of biodiesel, studies suggest that the equivalence ratio is closer to unity in certain regions of the combustion chamber which lead to higher local temperatures. But there is also evidence against this claim (using biodiesel in a gas turbine).

The book finally discusses reduction and control techniques for emissions using biodiesel such as use of EGR, use of fuel additives in biodiesel, low temperature combustion and delaying injection timing,

2. NATURAL GAS VVA

2.1 Baseline engine model

GT -Power is an engine performance simulation software used across vehicle manufacturers and engine companies to predict various output viz. power, torque, volumetric efficiency, turbo performance and so on. The model discussed for this work is representative of Cummins natural gas ISB 6.7 engine. It is an on-highway engine with 6.7-liter displacement and has peak torque of 560 ft-lbs. at 1600 rpm rated speed. The 1-D model is representative of the architecture of the engine, which is spark ignited, turbocharged, inline 6-cylinder engine with a charge air cooler.

Figure 2: 1-D model of engine [13]

The model is computationally efficient model to predict engine performance between the torque range of 25 ft-lbs. to 560 ft-lbs.

One of the limitations of the model however is that the model is not calibrated using the actual engine data. It has a pre-defined fixed heat release rate which might get validated with the actual engine results.

The inputs of EGR fraction, boost pressure targets and friction mean effective pressure values were initially provided by Cummins for a few torque values and the remaining values were obtained by interpolation.

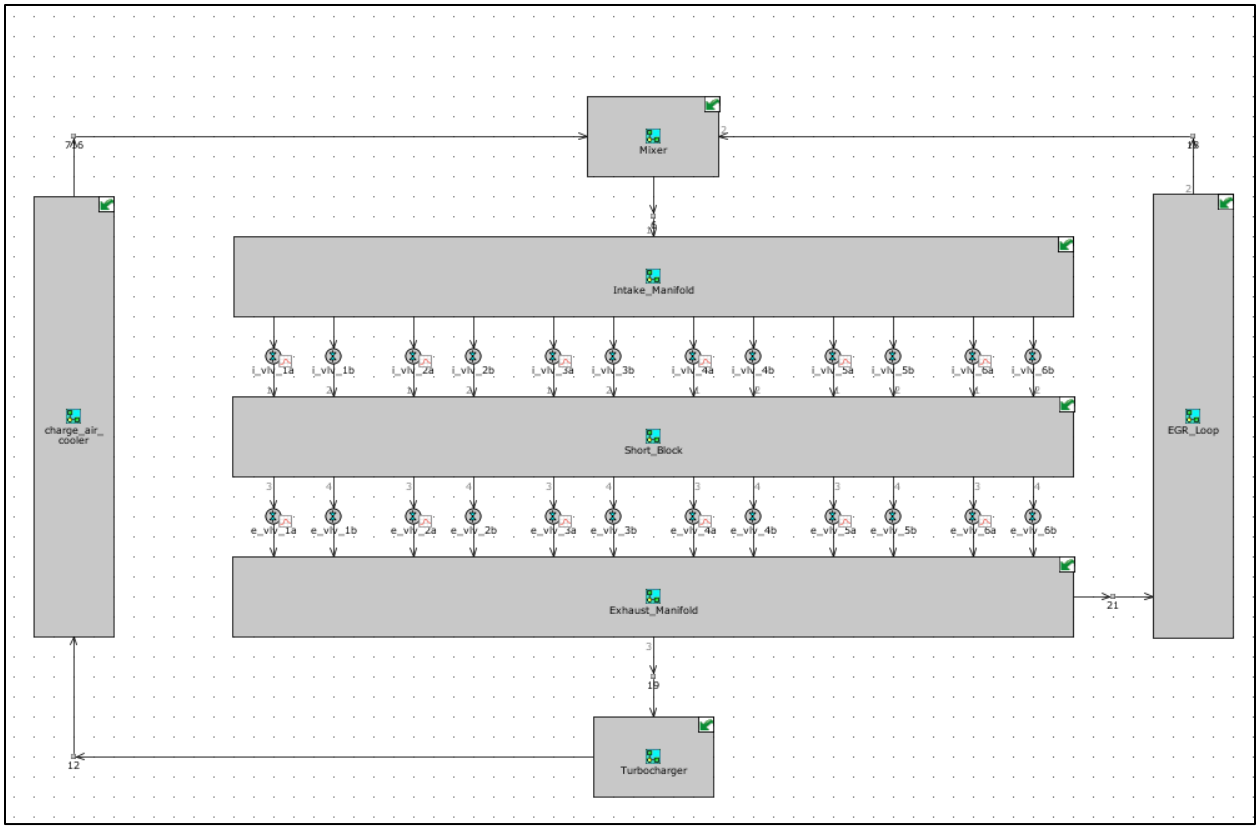

Figure 3: Engine model architecture

Figure 3 depicts top-level architecture of the model and following are the main building blocks –

Intake manifold: this block defines the connections between engine cylinder block (short block) and the mixer (air-fuel intake)

Short block: this block defines the six cylinders, one of them being a master cylinder and others being slave i.e., combustion parameters explain one cylinder and others mimic the same.

Exhaust Manifold: this represents the split exhaust architecture of the stock engine, with only 3 cylinders connected to EGR. The block also represents the connection to wastegate turbine from all 6 cylinders

Mixer: this block houses the throttle controller which controls the throttle opening and the stoichiometry of air-fuel mixture

EGR loop: this block defines the connection to EGR and the EGR controller which defines percent EGR flow for each speed-torque case.

Charge Air Cooler: this block defines connections between intake throttle and compressor

Turbocharger: this block houses the 3rd controller, the wastegate controller which defines the opening of wastegate diameter.

The model has total three constraints or control hooks as below –

1. Boost pressure controller: this is a control hook that defines wastegate turbine opening and how much of boosting needed for the commanded torque

2. EGR fraction controller: this controller defines the fraction of EGR and how much of combusted gases are recirculated back to intake manifold

3. Torque controller: this control hook controls the throttle opening and air-fuel mixture to meet the required torque demands.

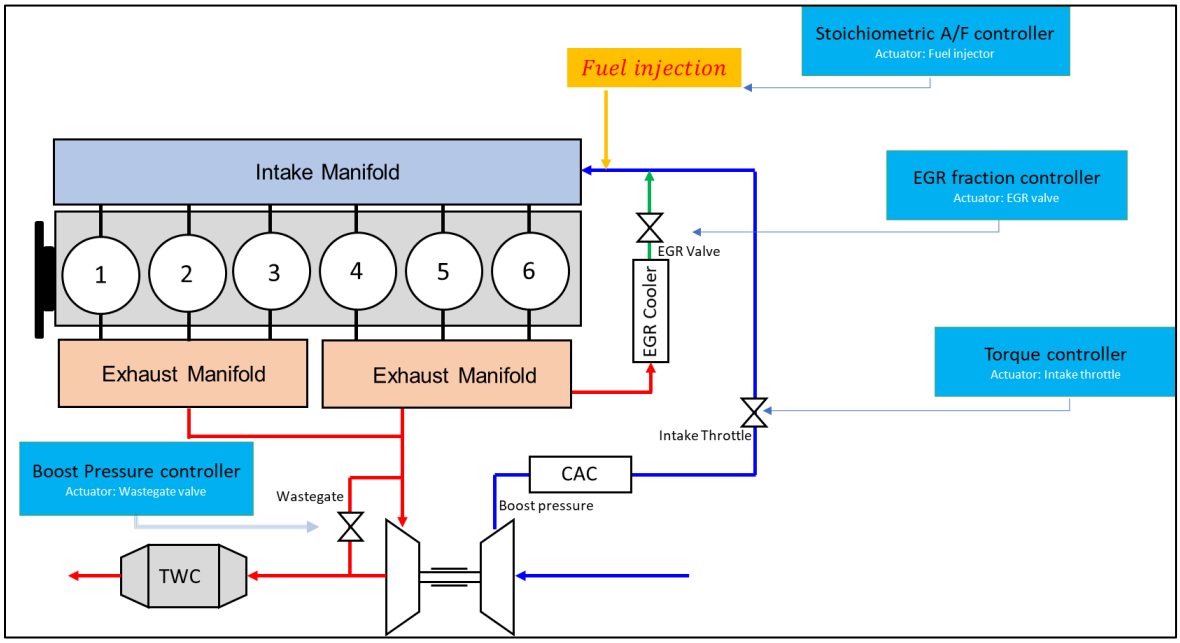

Figure 4: Engine schematic

2.2 IVC modulation

Intake valve modulation has been linked with optimizing volumetric efficiency of the engine by altering the effective volume available for combustion process inside the cylinder. Intake valve closure strategies discussed here are achieved by either advancing or delaying the intake valve closure timing, in degrees.

Unlike compression ignition engine, S.I engines have throttle intake system to control air-fuel inlet. Thus, the pumping losses in spark ignited engines are higher at low speeds due to the

presence of throttle valve that controls the intake of air-fuel mixture. IVC modulation techniques are one way to address the pumping losses at part loads for S.I. engines.

EIVC and LIVC reduce the volumetric efficiency, allowing the engine to operate with higher intake manifold pressures while maintaining stoichiometry, enabling reductions in the pumping work by bringing the pressures in the intake and exhaust manifold closer together.

2.2.1 Early intake valve closure (EIVC)

Intake valve closure happens at the end of intake stroke and start of compression stroke. Advancing the intake valve closure has typically resulted in more stable combustion, longer flame development period. Decreased effective compression ratio lowers IMEP and temp, decreases NOx emissions. [6]

For the simulation studies discussed in subsequent sections, intake valve was closed 20 degrees in advance as compared to the baseline position for 1st run and then advancing by 20 degrees till a final IVC run with intake valve closed 150 degrees earlier compared to baseline.
The intake valve closure profiles for EIVC are as shown in fig 5.

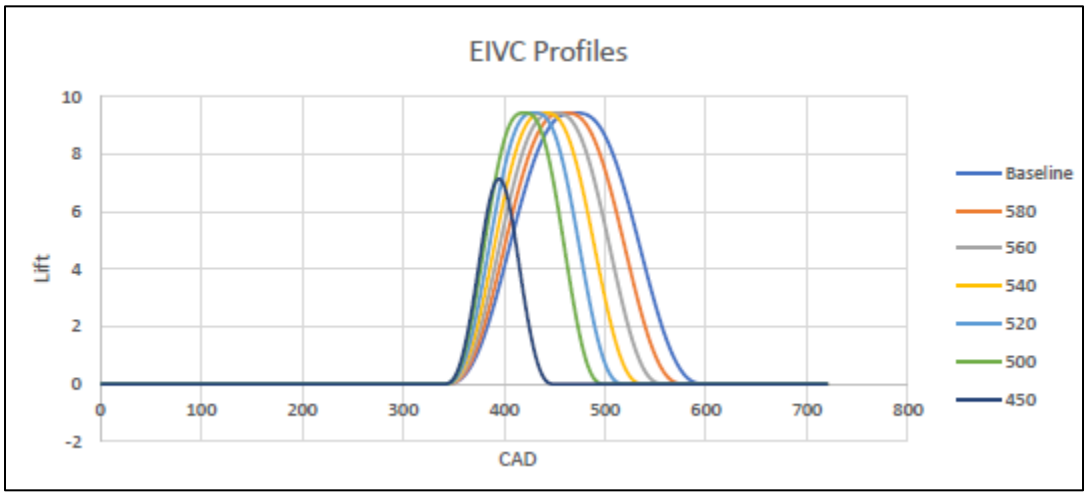

Figure 5: EIVC profiles

2.2.2 Late intake valve closure (LIVC)

In the case of LIVC, it is achieved by delaying the closure of intake valve at the end of compression stroke. Delaying the intake valve closure helps in significant reduction in pumping losses at partial load (approx. 40%) with minimal torque reduction, increased high-speed volumetric efficiency

due to greater charge volume and allows variable compression/expansion ratio (approx. 20% decrease in BSFC). [6]

Late intake valve closure was run in succession to EIVC strategy as explained above. The intake valve closure was delayed here from the baseline position (600 CAD) gradually by 20 degrees as shown in fig 6. LIVC700 was considered an aggressive LIVC strategy.

It is expected that there will be some back flow of the combusted air-fuel mixture in the intake manifold, because of delay in closing the intake valve at the end of compression stroke. This would result in reduction in temperature of combusted gas and result in lower NOx.

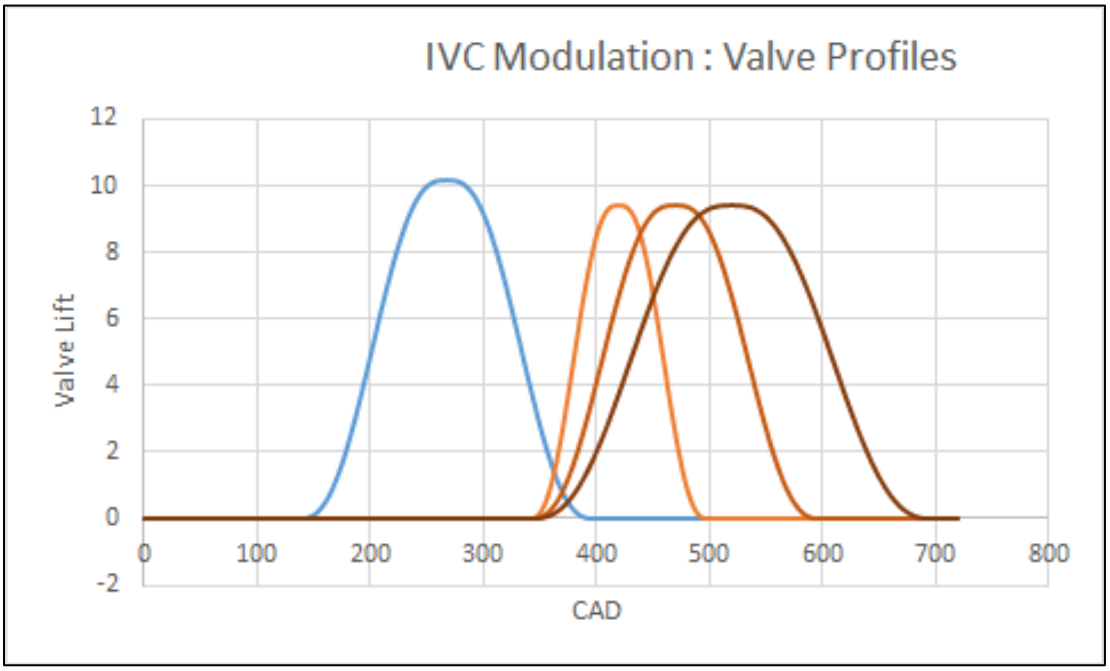

Figure 6: IVC profiles

The naming convention followed in the analysis is shown in Figure 6.

The baseline profile and intake timing are named IVC CAD 0 degree. All other variable valve timings are named with respect to the baseline. For example, for advancing the intake valve closure by 100-degree CAD, the profile is named *IVC Neg 100*, and delaying valve closure timing by 100-degree CAD is named *IVC Positive 100*. The GT Power simulation is run for a sweep of IVC timings from IVC Negative 150 to IVC Positive 100, although in the following figures, only a select few have been plotted to see the trend and clear representation.

The IVC modulation strategies were implemented for a torque range of 25-125 ft-lbs. (low torque region).

3. RESULTS AND DISCUSSION

3.1 Baseline results

Baseline model was initially run for entire high torque range (between 354 ft-lbs. to 664 ft-lbs.) to understand model behavior and any convergence issues.

The parameters that were studied were:

Open cycle efficiency – is a measure of ability of the engine to transfer the products of combustion in and out of the cylinder. It is expressed as [14]

$$\eta_{open} = \left[1 + \frac{PMEP}{GIMEP}\right] - (10)$$

Closed cycle efficiency – is a measure of combustion efficiency and thermodynamic efficiency of the engine, closed cycle being the time when intake and exhaust valves are closed. It is expressed as

$$\eta_{closed} = [\frac{\text{GIMEP}}{\frac{m_{fuel} * Q_{LHV}}{D}}] - (11)$$

Mechanical efficiency – is defined as efficiency of the engine to transmit the work generated by the expanding gases in the cylinder to the output shaft and is given as

$$\eta_{mechanical} = \left[\frac{BMEP}{BMEP + FMEP}\right] - (12)$$

Brake thermal efficiency – is defined as engine output divided by fuel energy input [Stanton] and is expressed as

$$\eta_{thermal} = \left(\eta_{open} * \eta_{closed} * \eta_{mechanical}\right) - (13)$$

P-V diagrams – pressure Vs volume diagram in logarithmic scale is referred for getting graphical representations of open cycle efficiency, closed cycle efficiency and pumping loop. Though P-V diagrams do not include temperatures to give a clearer picture of thermal efficiency, it leads to overall idea about the gas exchange and engine efficiency

Brake specific fuel consumption – it is a measure of efficiency of an engine which burns fuel and produces power at the crankshaft. It is expressed as

$$BSFC = \frac{m_{fuel}}{P_e} - (14)$$

Fiction mean effective pressure – is the mean effective pressure due to friction losses.

As such there were a few outliers observed in the data for efficiency plots. Baseline model showed 3 outliers in the data for open cycle efficiency, closed cycle efficiency and mechanical efficiency and were resolved by following debugging techniques

- Target Boost Pressure (Compressor Output Pressure in DOE setup) changed from constant values to proportional lower values for lower target torques
- Friction model modified – the Chen-Flynn friction correlation model is used to calculate FMEP of the model and it is calculated as below (X-Engineer.Org)

$$FMEP_{engine} = afmep + B * p_{max} + C * S_f + D * S_f^2 - (15)$$

Where, afmep = constant and accounts for auxiliary friction

B = constant, which accounts for the load effect of the engine (in-cylinder pressure)

P_{max} = maximum cylinder pressure

C, D = constants, which accounts for the effect of the engine speed (as a quadratic law)

S_f = Speed factor

The value of afmep was changed to 1bar for all cases

Main | Initial | Short_block | Independent_variable | Initialization | DOE_Setup | Test Cell Data | Short Block | All

Parameter	Unit	Description	Case 1	Case 2	Case 3	Case 4	Case 5
Case On/Off		Check Box to Turn Case On	☑	☑	☑	☑	☑
Case Label		Unique Text for Plot Legends					
afmep	bar	For the friction model	1	1	1	1	1
bfmep		For the friction model	0	0	0	0	0
bore	mm	Cylinder Bore	107	107	107	107	107
cfmep	bar/(m/s)	For the friction model	0	0	0	0	0
clnt_ot_t	K	Coolant outlet temperature(K)	368.8	368.8	368.8	368.8	368.8
CR		Compression Ratio	12.7	12.7	12.7	12.7	12.7
IVC		Intake Valve Closing (Cycle Start)	-120	-120	-120	-120	-120
oil_t	K	Oil temperature(K)	394.9	394.9	394.9	394.9	394.9
stroke	mm	Cylinder Stroke	124	124	124	124	124

Figure 7: Friction model

Convergence issues were faced during the initial trials for the three controllers, but the model converged once above-mentioned issues were solved, indicating they stemmed from the above-mentioned issues.

3.2 IVC results

As stated in previous section, IVC modulation simulations were run for low torque region and were aimed at torque range below 125 ft-lbs. with focus on pumping losses at low loads.

Starting from the fuel efficiency and brake thermal efficiency, both EIVC and LIVC showed fuel consumption benefits in the simulated torque range. As seen in Figure 8, the fuel flow rate decreases with respect to baseline with aggressive strategies showing the maximum benefits (IVC Neg 120 with 9% reduction in fuel flow rate). The values shown are based on normalized data.

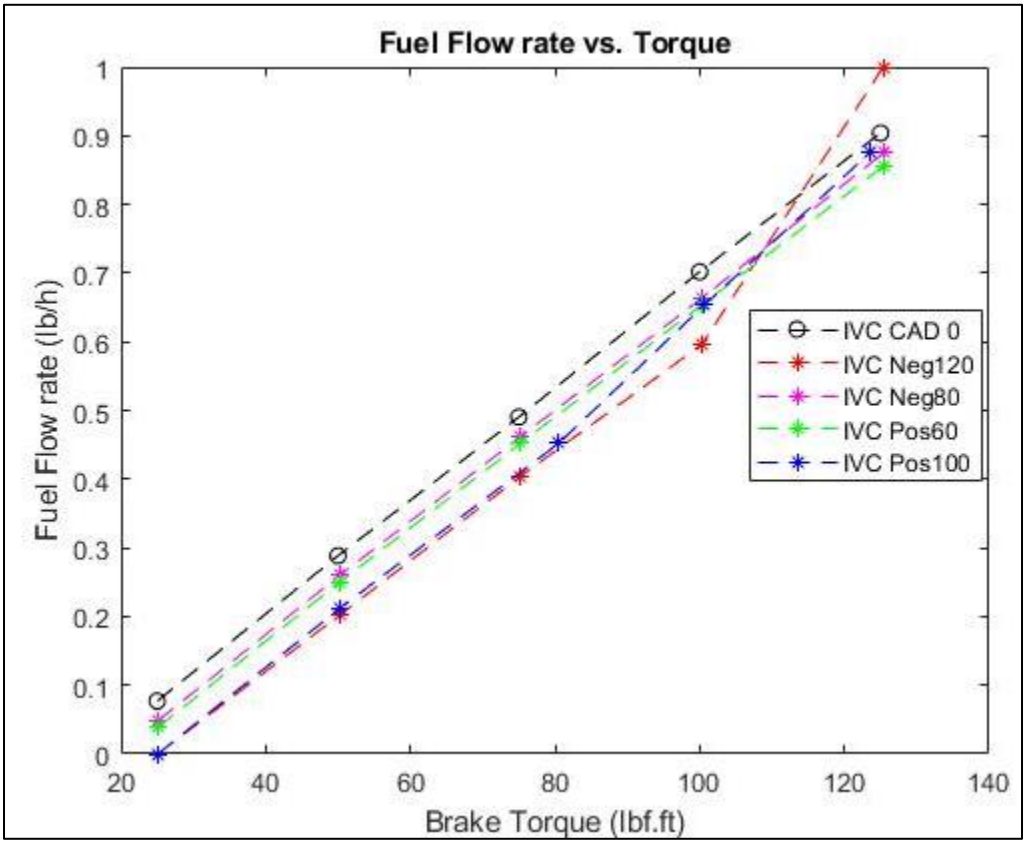

Figure 8: Fuel Flow Rate vs. Torque.

The corresponding Brake Thermal Efficiency improvements were seen in Figure 9 with a maximum 3% increase for aggressive IVC Neg 120. These values are normalized as well.

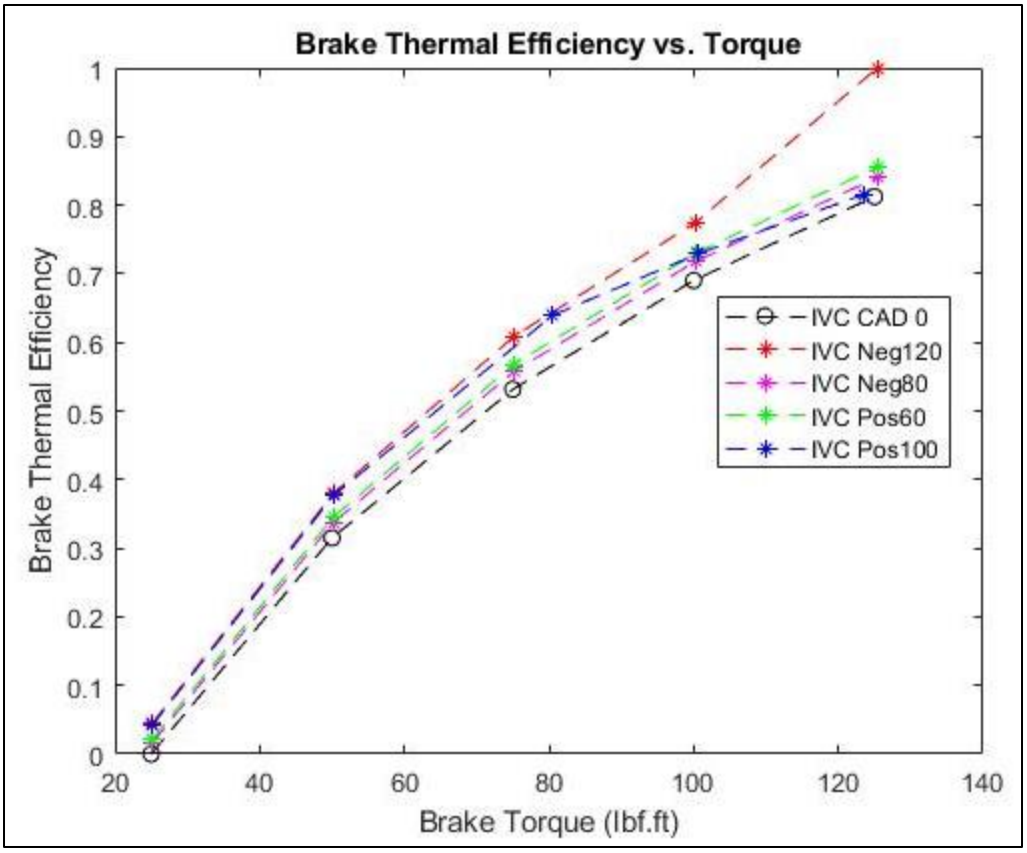

Figure 9: BTE vs. Torque.

The fuel consumption benefits were most significant at low loads since stock engine pumping losses are the maximum at low loads. The benefits tend to reduce as the load is increased. This can be seen in BSFC plots (normalized values) in Figures 10 and 11.

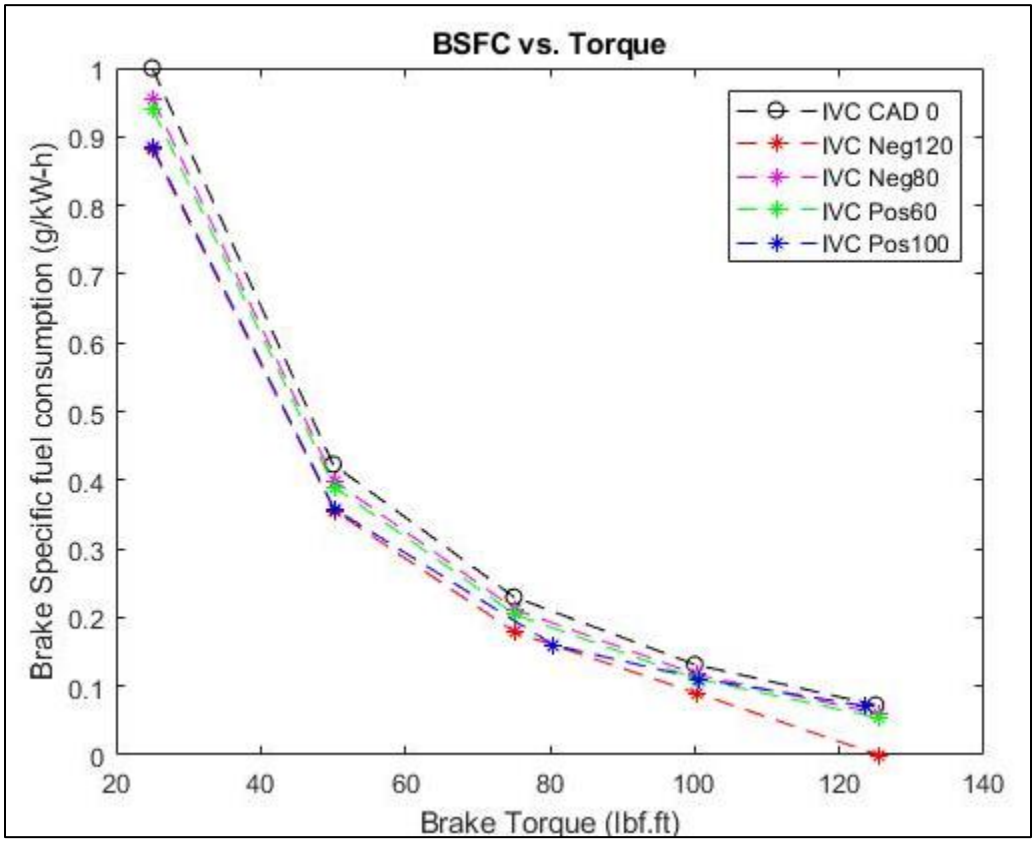

Figure 10: BSFC Vs Torque

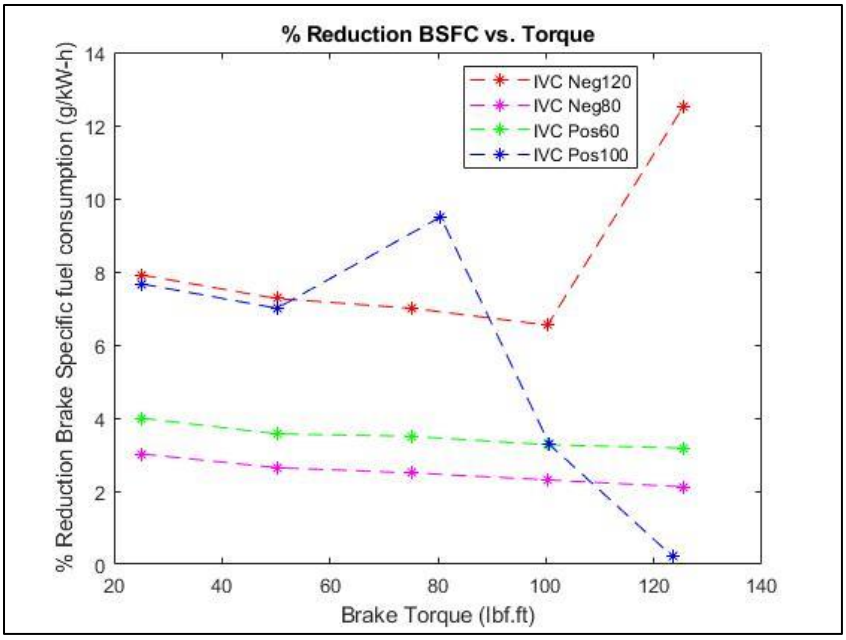

Figure 11: Percent reduction BSFC Vs Torque

From Figure 12, where in desired torque vs actual torque is plotted, it was seen that the torque demand is met for all IVC timings and the entire low load torque range, with the adjusted boost pressure inputs. This data needs to be validated with engine data, as discussed in section 6 of this document.

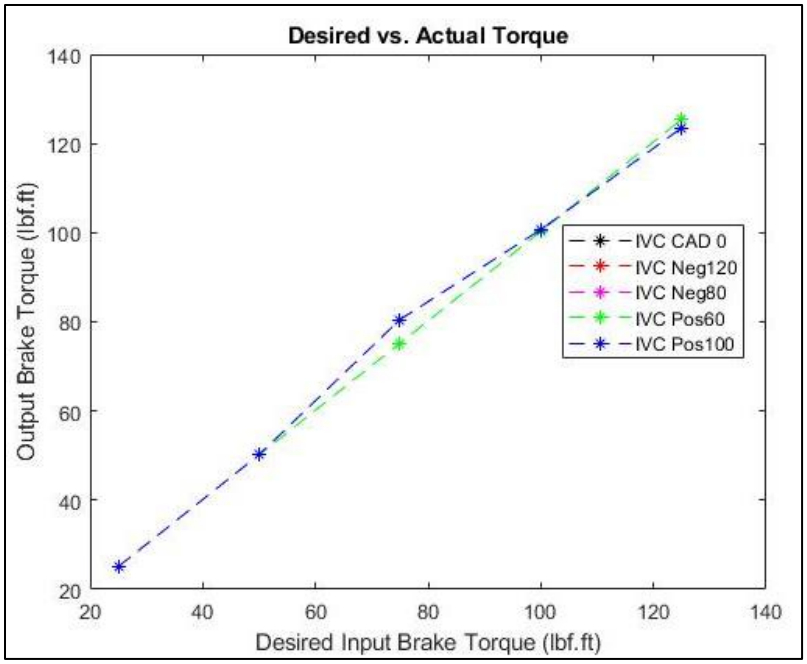

Figure 12: Desired torque Vs actual torque

The EGR fraction demand was met for most of the torque values except for the aggressive LIVC case IVC Pos 100 at torques above 50 ft-lbs. wherein the EGR valve was at fully open condition, the diameter being fully open. The corresponding EGR valve operation can be seen in Figure 13.

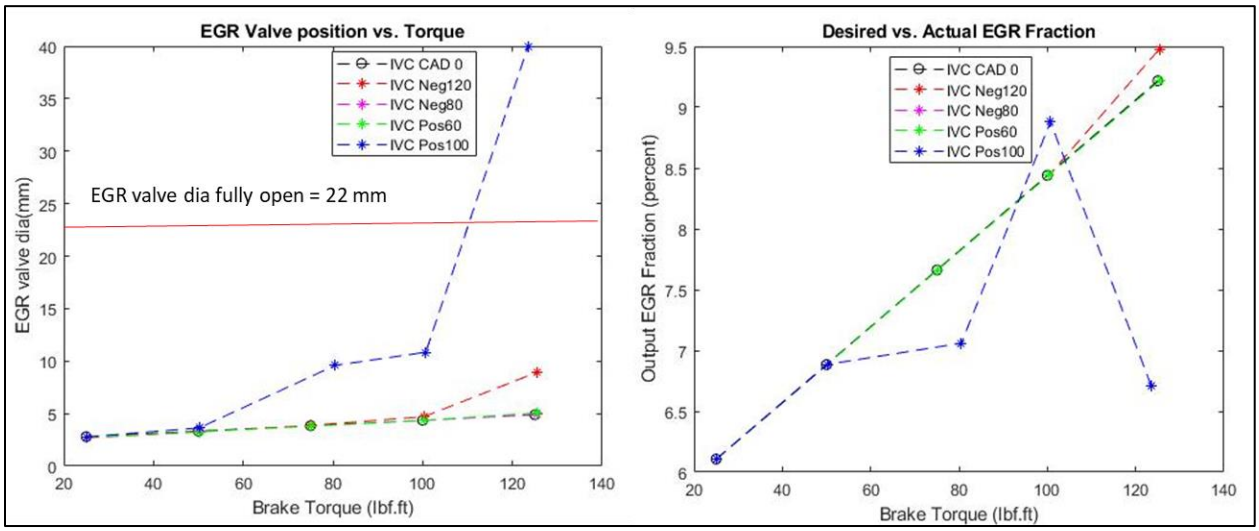

Figure 13: EGR fraction

As noted previously, IVC modulation has the advantage of reducing the volumetric efficiency (see Figure 14), allowing the engine to operate with higher intake manifold pressures (see Figure 15), which further results in reduced air and fuel flow and in turn reduced charge flow. Higher intake manifold pressure further results in reduced pumping loop.

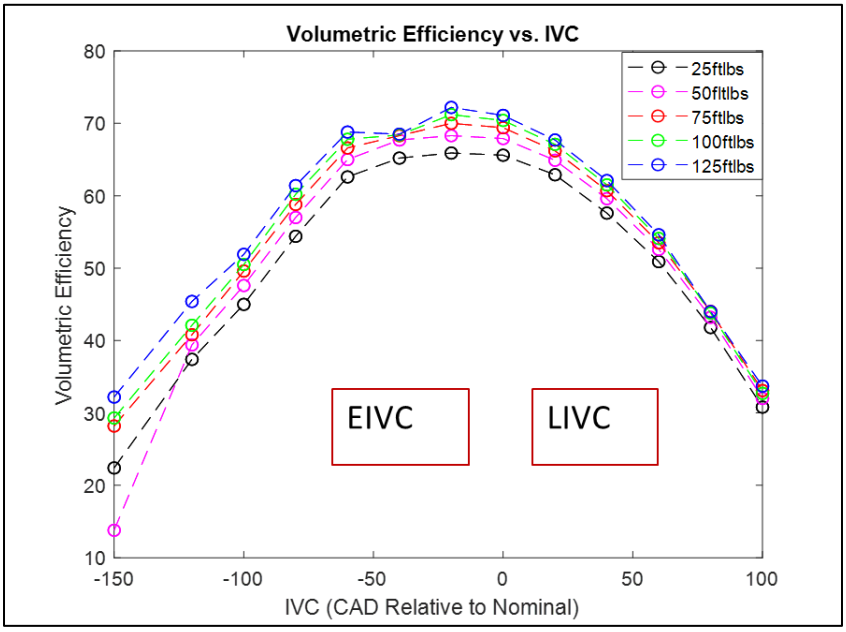

Figure 14: Volumetric efficiency Vs IVC

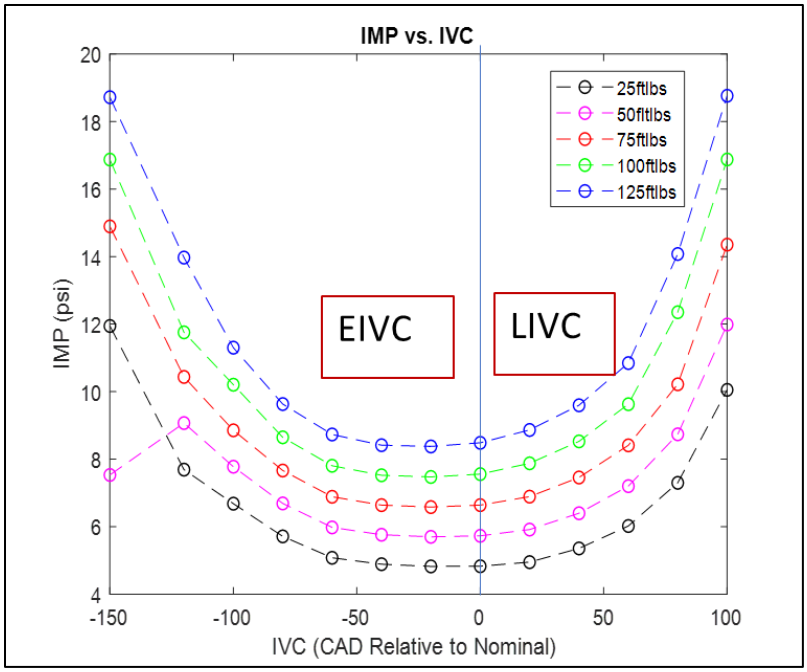

Figure 15: IMP Vs IVC

As discussed above, higher intake manifold pressure helped to reduce the pumping loop (see Figure 16 which shows PV diagram for one case). It further led to increase in the open cycle efficiency (see Figure 17).

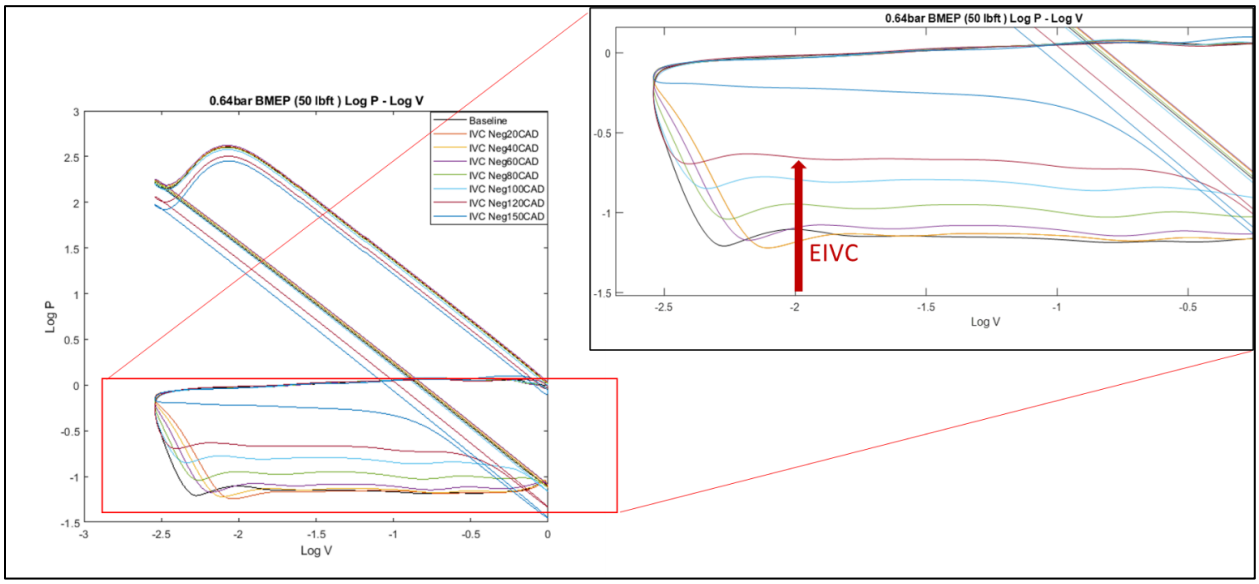

Figure 16: PV diagram for 0.64 BMEP

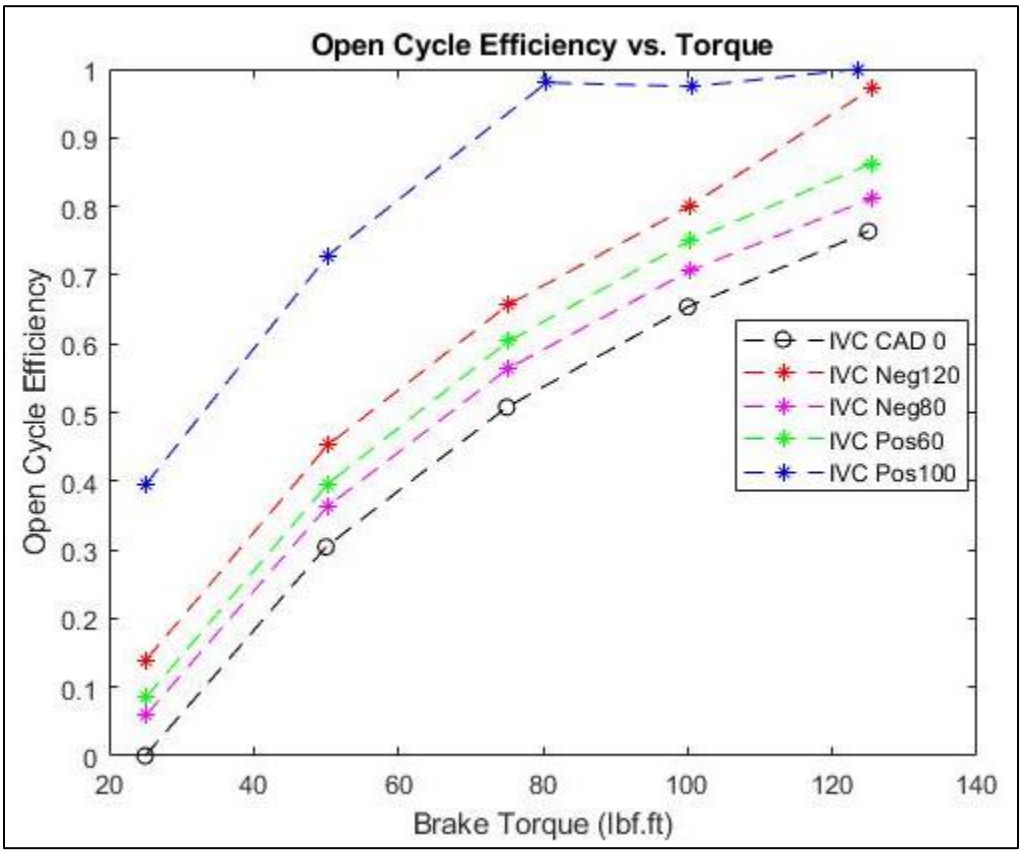

Figure 17: OCE vs torque

The in-cylinder pressure and temperatures represent the combustion efficiency and they dropped as IVC modulations were made more aggressive. However, this needs to be validated with engine data, which will be discussed in section 6 of this document.

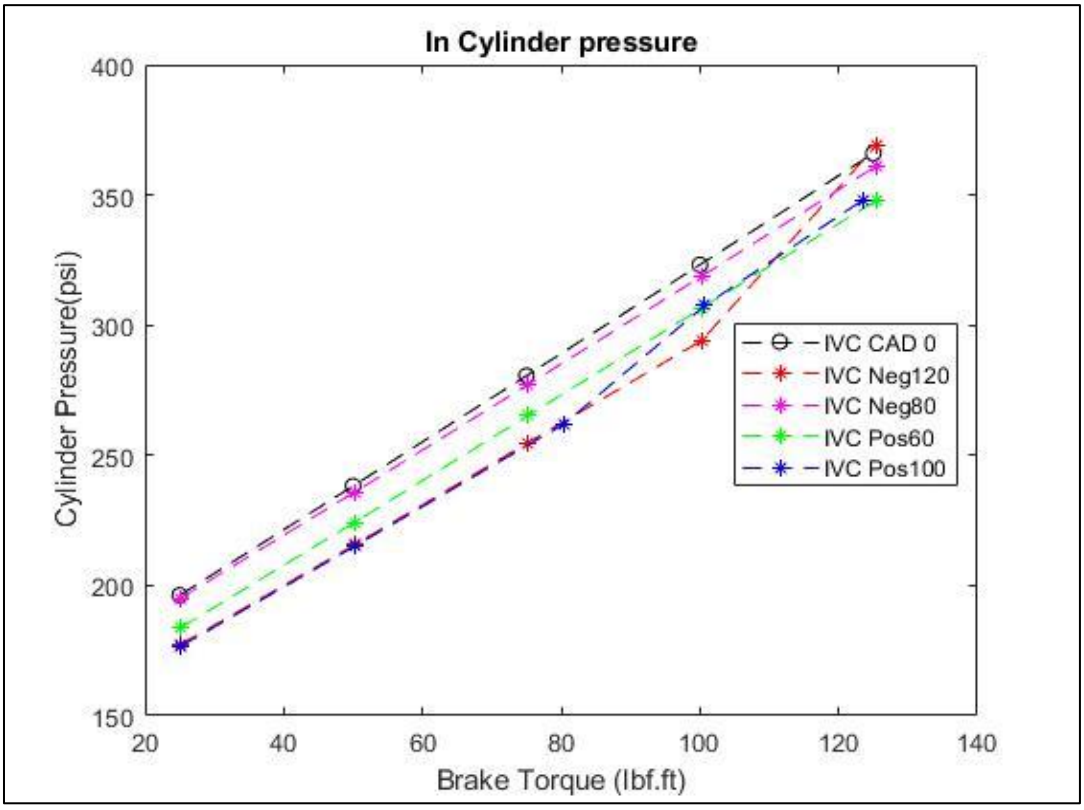

Figure 18: In-cylinder pressure at SOC

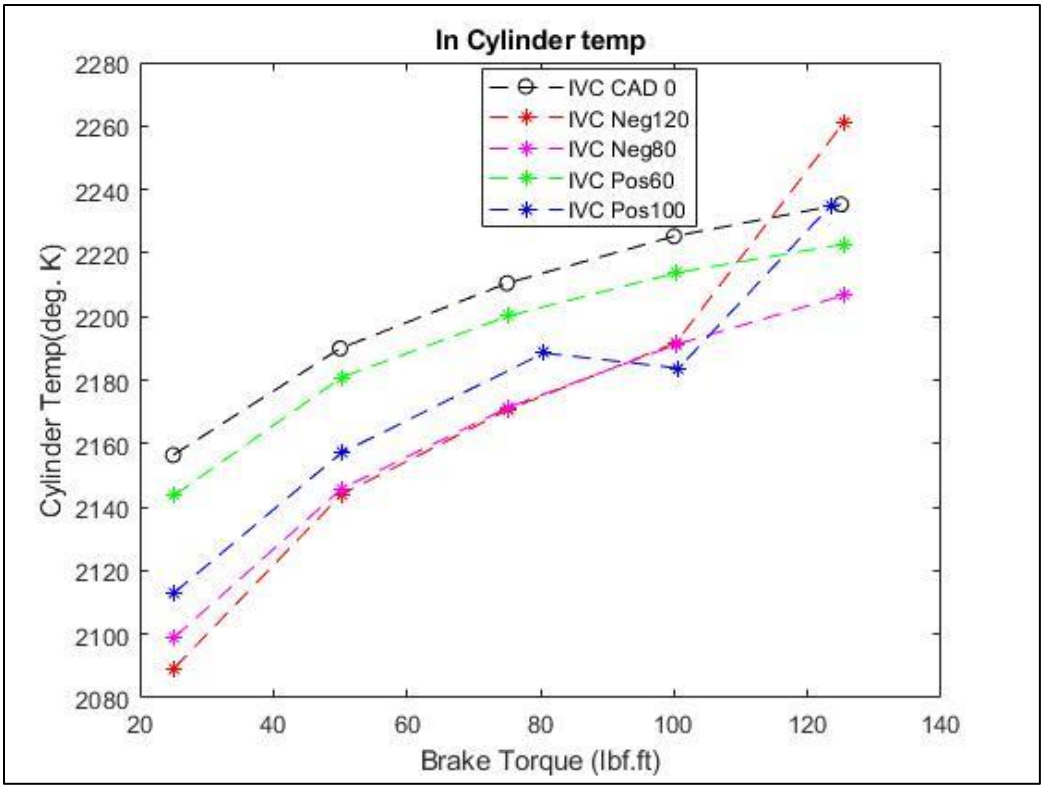

Figure 19: In-cylinder pressure

The effective compression ratios represent the ratio of effective volume at IVC to the total volume at TDC, which is another way to represent the breathing capacity of the engine other than volumetric efficiency. It was observed that ECR were reduced as IVC were either delayed or advanced as shown in fig. 20. However, the ECR values as low as 2 seem less realistic and it will need to be seen how these values get affected with a more advanced GT-power model with realistic heat release data imposed on it.

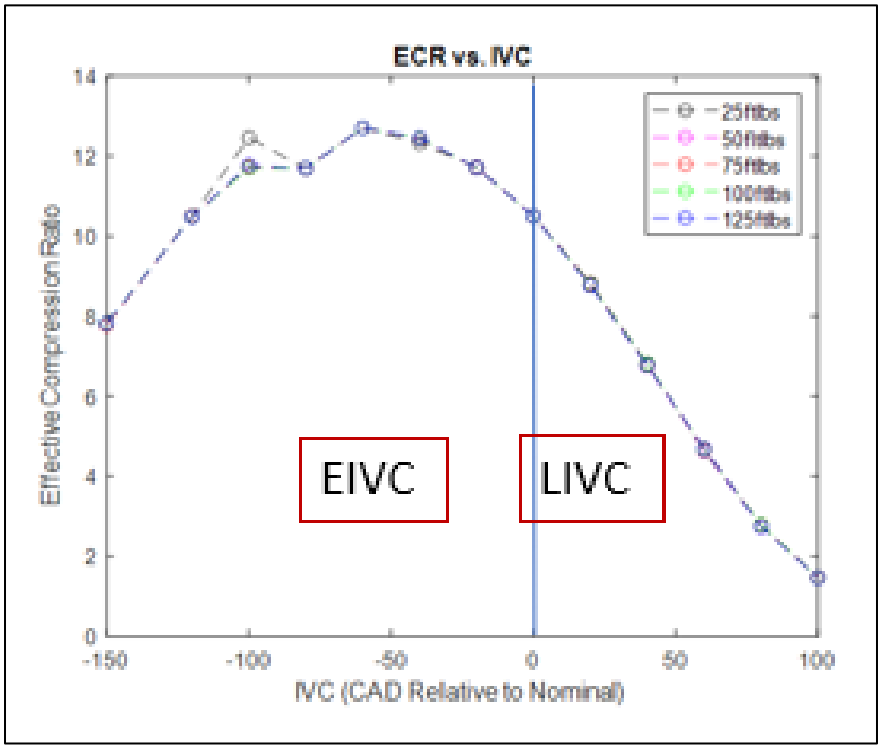

Figure 20: ECR

4. BIODIESEL

4.1 Project Motivation

Prior to mid-2000s, most heavy-duty diesel engines were equipped with EGR systems to meet the NOx emissions standards. Starting mid-2000s, with Euro V and EPA 2007 equivalent emission norms which mandated stringent limit on NOx emissions (0.2 g/bhp-hr.), thus requiring SCR systems along with DOC and DPF. In the United States, SCR systems were introduced by most engine manufacturers in 2010, to meet the US EPA NOx limit of 0.2 g/bhp-hr. for heavy-duty engines[16]. It needs to be assessed that how these modern after-treatment systems behave when biodiesel fuel is being used in the engine that is tuned for diesel fuel.

Specifically, between 1994 and 2006, US EPA started making stringent emission standards for on-road heavy-duty diesel engines on reducing NOx emissions. During this period, NOx emission requirements dropped from 5.0 g/bhp-hr. to about 2.4 g/bhp-hr., which most engine manufacturers met with using EGR only exhaust systems. In early 2007, emission limits for NOx and PM dropped considerably, with NOx limit being 0.2 g/bhp-hr. (0.27 g/kWh) to be brought between 2007 and 2010 making most manufacturers to work on design of reducing catalysts (SCR) in addition to existing technologies to control emissions by making changes in in-cylinder combustion and increasing EGR levels[16] .

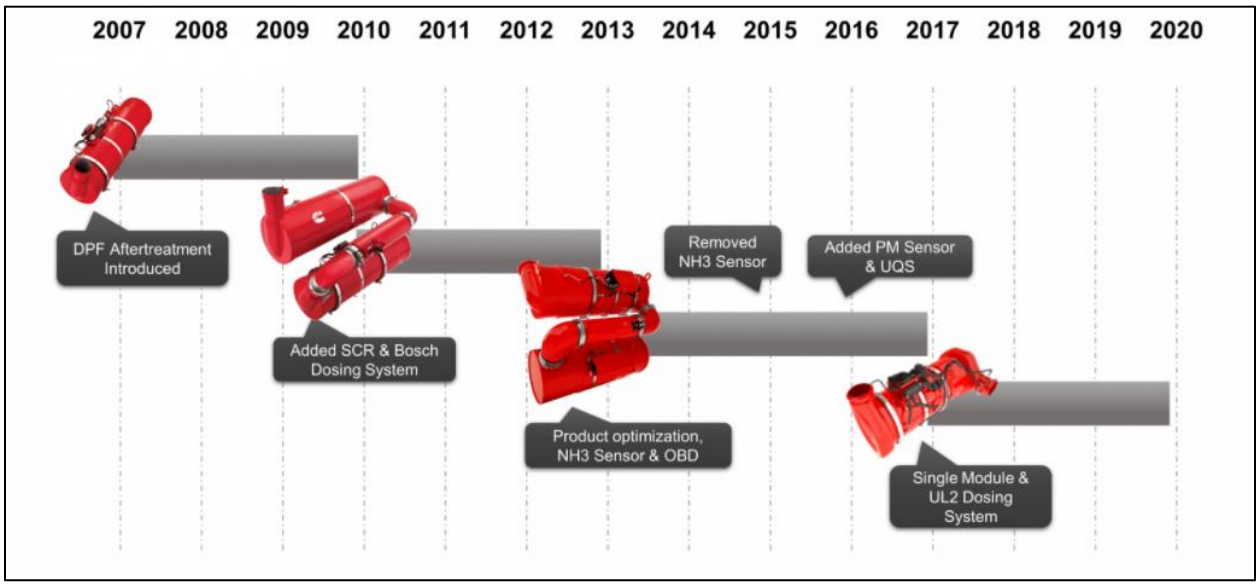

Figure 21: After-treatment system development over the years [17]

Similarly, around the globe the equivalent emission norms made it compulsory to switch to adding SCR catalysts in the aftertreatment structures. For example, in Europe, Euro V standards for heavy-duty diesel engines around 2008 timeframe required NOx emissions to be dropped from the Euro IV level of 3.5 g/kWh to 2.0 g/kWh [18].

Thus, it became important to study the effect of using biodiesel fuel on these post EPA 2007/Euro V complaint engines equipped with modern after-treatment systems.

4.2 Experimental Setup

The outline of the Biodiesel project work was to study biodiesel fueled engine with a single module after treatment system, performance of the same against the diesel fuel and the resulting emissions from the same. In addition, another aim was to understand the impact of using varying biodiesel blends on modern after treatment systems used in diesel engines in on highway applications. As previously stated, a modern-day diesel after treatment system would refer to the one equipped with NOx reducing catalyst.

The engine used for this project was Cummins X15 efficiency series (2017) on highway engine for heavy duty applications. The after-treatment system on the engine was Cummins single module side inlet side outlet (SISO) after treatment system with DOC + DPF + Urea doser and mixer + SCR ASC architecture. The engine has maximum power output of 400 hp -500 hp and 1450 ft-lb to 1850 ft-lb peak torque.

The engine test bed has Power Test heavy-duty AC regenerative dynamometer rated at 670 hp and is capable of real world and certification-type drive cycles (including transient cycles viz. FTPs).

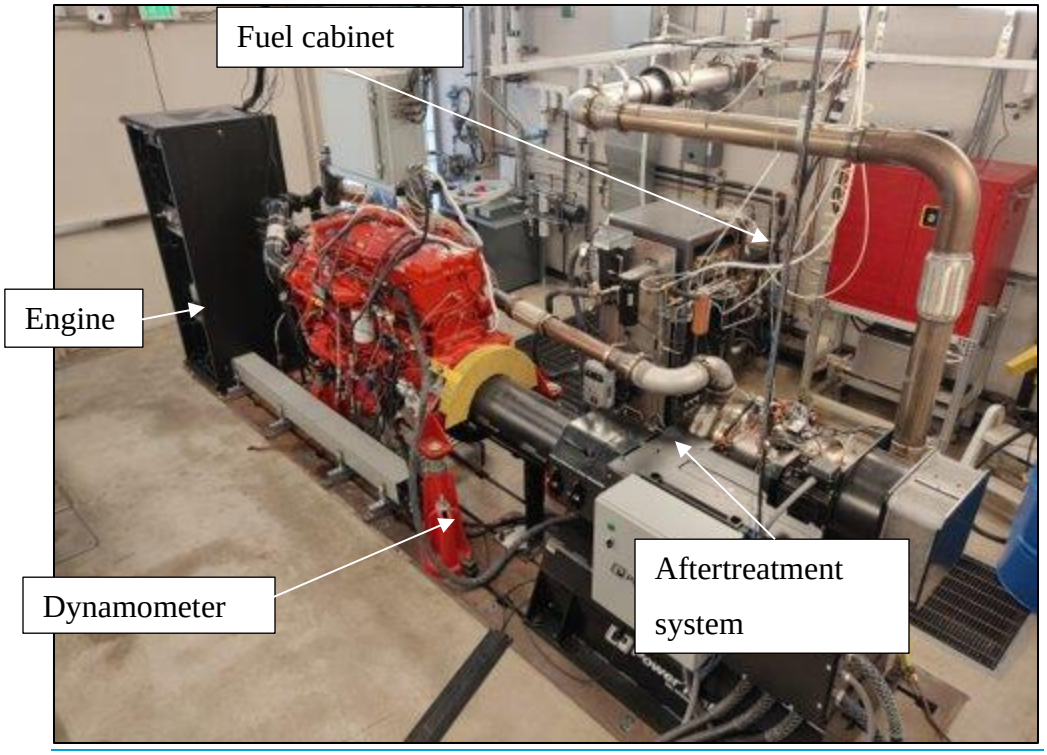

Figure 22: Engine test bed

As shown in above image, dynamometer and engine mounted centrally and after treatment system is mounted on the side, with the help of exhaust pipe and elbows. The tailpipe is connected to building exhaust.

After treatment system is equipped with stock sensors as listed below –

- Temperature sensors
  - At inlet of DOC
  - At inlet of DPF
  - At outlet of DPF
  - At inlet of SCR
  - At outlet of SCR
- PM sensor: located on a sensor table plate mounted above DPF
- NOx Sensors: Cummins stock NOx sensors
  - Engine Out NOx: located at outlet of Turbo
  - Tailpipe Out NOx: located at outlet of SCR
- Pressure sensors:

- Pre and post turbo
- Across DPF

- ECM Calculated/Tabular Measurements:
  - Fueling
  - Air Flows
  - Injection Timing
  - Turbine Speed
  - EGR Position

Some of the above sensors are as highlighted in the image below:

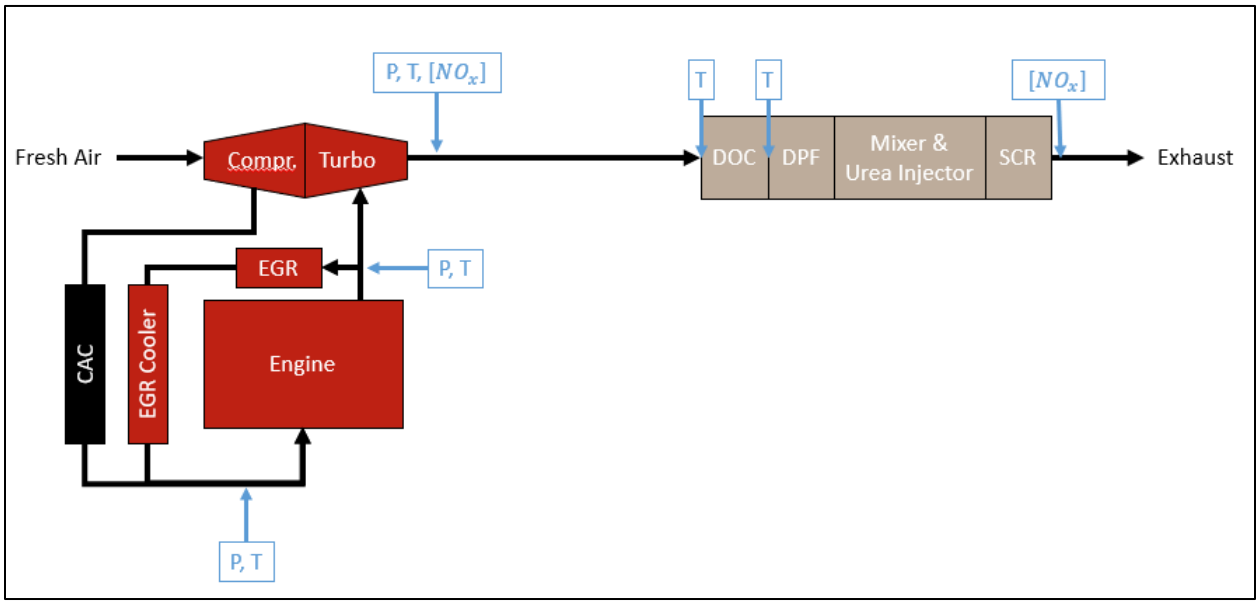

Figure 23: Sensor locations

4.3 Test Procedures

4.3.1 Diesel – Biodiesel switching

The first pre-requisite for the testing included an arrangement for frequent switching between diesel to a biodiesel blend as there was a common fuel reservoir being used for the tests. This required a standardized process to be followed. Following were the steps involved while doing the fuel switching –

- Burn the existing fuel in the fuel bucket until it was empty, then turn off the fuel lift pump.

- Remove the fuel bucket and empty it by wiping it to clean off any residue of the previous fuel. Then replace the bucket.
- Switch the fuel return valve to purge the fuel in the fuel lines.
- Then the fuel bucket was filled with new fuel blend.
- Turn on the fuel lift pump and then run the lift pump until it went nearly dry and then turn off the lift pump
- Lastly, switch valve to fill the fuel bucket with new blend and run the steady state point. The chosen steady state point was 1000 rpm and 600 ft-lbs. to compare and confirm new blend was running through the engine.

4.3.2 RMC set points

As the last leg of testing, steady state points were run for each blend. The tests were run based on 13 Supplemental Emissions Test (SET) points defined by US EPA originally defined for heavy duty engines and speed torque conditions for the engine were based on the torque curve for the test engine, as defined in the table 2 below.

Table 2: RMC set points

ID	Speed	Torque
	[RPM]	[ftlb]
A25	1148	388
A50	1148	775
A75	1148	1163
A100	1148	1550
B25	1375	388
B50	1375	775
B75	1375	1163
B100	1375	1550
C25	1603	378
C50	1603	756
C75	1603	1134
C100	1603	1512

The SET points are defined over low speed to high speed and approximately 25% throttle to a 100% throttle condition. The points in the table above are as per the advertised torque curve developed for diesel. Steady state testing was done at non-idle RMC set points.

The testing was done such that each steady state point was run till the engine ECM parameters (engine out and tailpipe out NOx, DPF out temperature and fueling rate) showed stabilized values and subsequently data was recorded for a duration of 300 seconds.

Subsequently, torque curves were developed for biodiesel blends B20, B50 and B100 by running the engine at 100% throttle and taking a speed sweep from 600 rpm to 1800 rpm. These torque curves were then overlapped and compared with that of the available torque curve for diesel. In developing the torque curves, the only control hook that was used for percent throttle as

controlling the fueling by overriding the fueling rate in engine ECU was not possible. This is discussed in detail in the next section.

As a small subset of the experiments, density analysis was also done for diesel and biodiesel blends to verify the fuel densities to be in the range that was expected. This was done by simply weighing each blend using a container with known volume. Two weighing scales with accuracies of 10 g and 0.1 g were used.

5. RESULTS AND DISCUSSION

5.1.1 Torque curve developments:

The test engine was developed for the diesel fuel and thus the advertised torque curve was developed for the same. As biodiesel has lower density compared to diesel, the fueling rates increased for biodiesel compared with diesel, to meet the same torque. To understand how this influences on the torque limits, and torque envelopes for biodiesel, a small set of experiments were run with each biodiesel blend.

As stated in previous section, torque curves were generated by running a speed sweep from 600 to 1800 RPM with 100% commanded throttle at a rate of 1 RPM/s. Following figure shows the envelopes thus developed for diesel (blue color), B20 (orange color), B50 (grey color) and B100 (yellow color). The RMC set points are shown in filled red squares and the advertised torque curve is shown in black dotted line.

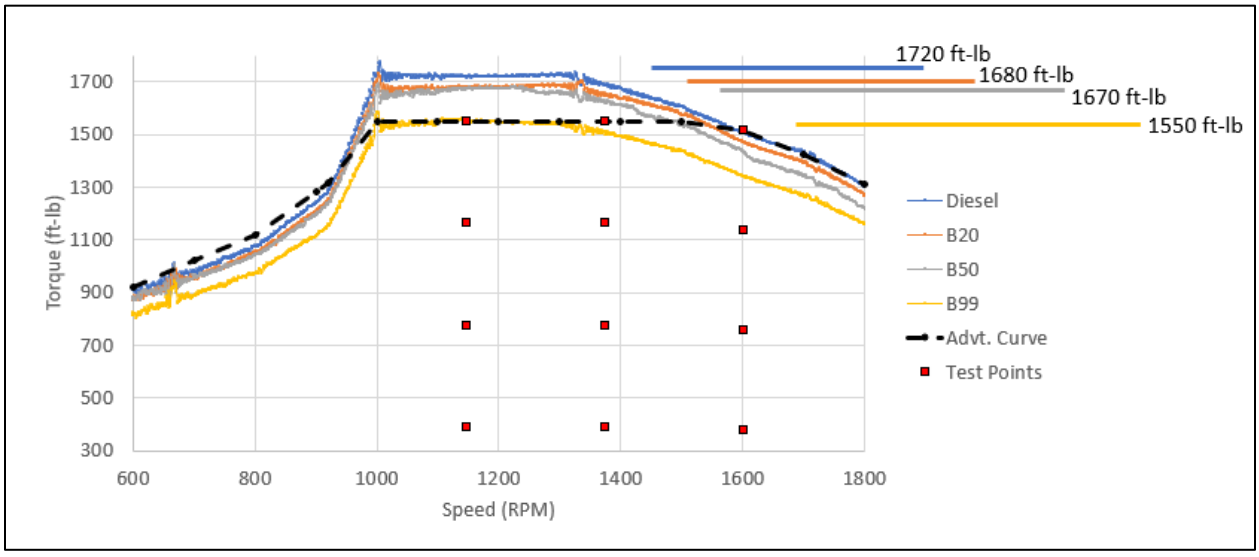

Figure 24: Torque curve envelopes

It was observed that peak torque was around 40 ft-lb less for B20 compared to diesel (2% lower), peak torque was around 50 ft-lb less using B50 compared to diesel (3% lower) and peak torque was around 170 ft-lb less using B100 compared to diesel (10% lower).

5.2 Steady state testing

5.2.1 RMC set points

Steady state trials focused on data logged by stock sensors and engine ECU. The data for each point was logged for 300 seconds and values used in the plots below are mean values for each parameter.

As seen in fig. 25 and fig. 26, engine out and tailpipe out NOx significantly increased with increase of biodiesel blend percent. It was also noted that NOx appeared to increase non-linearly with percent biodiesel. For biodiesel blends B20 and B50, NOx values observed are nearly the same or even lower for some conditions. B100 NOx is significantly higher than Diesel, B20, or B50.

Engine out and tailpipe out NOX values are normalized.

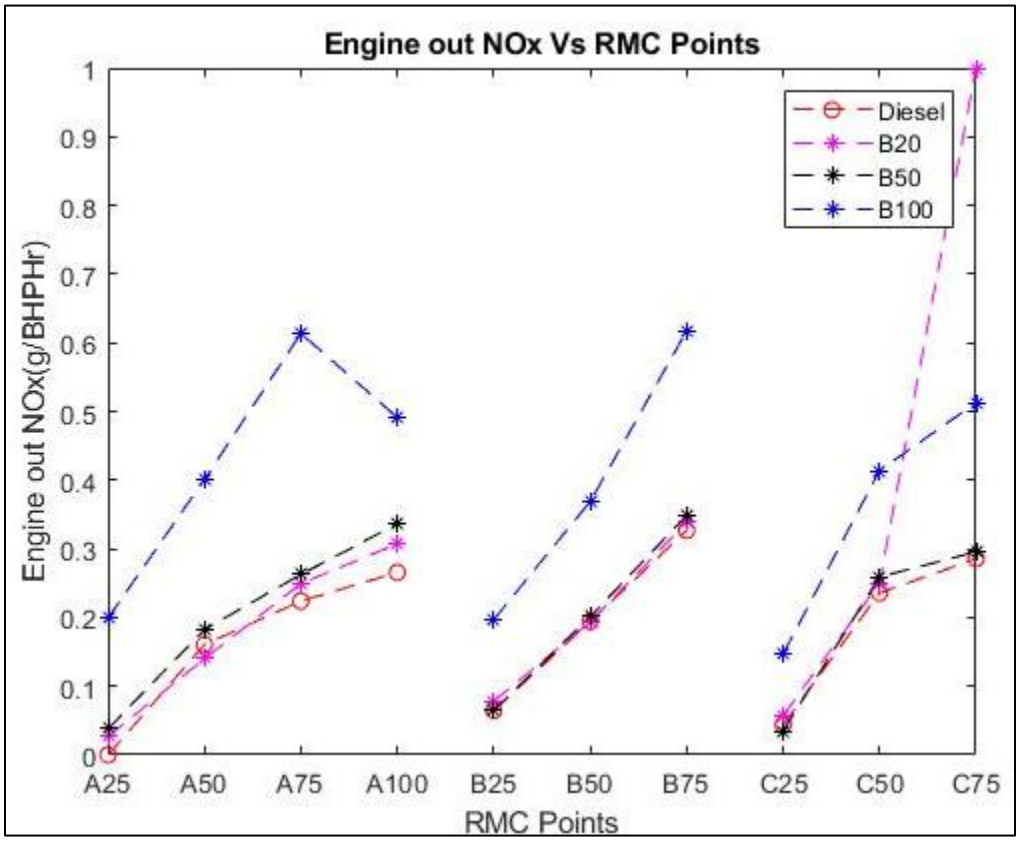

Figure 25: Engine out NOx

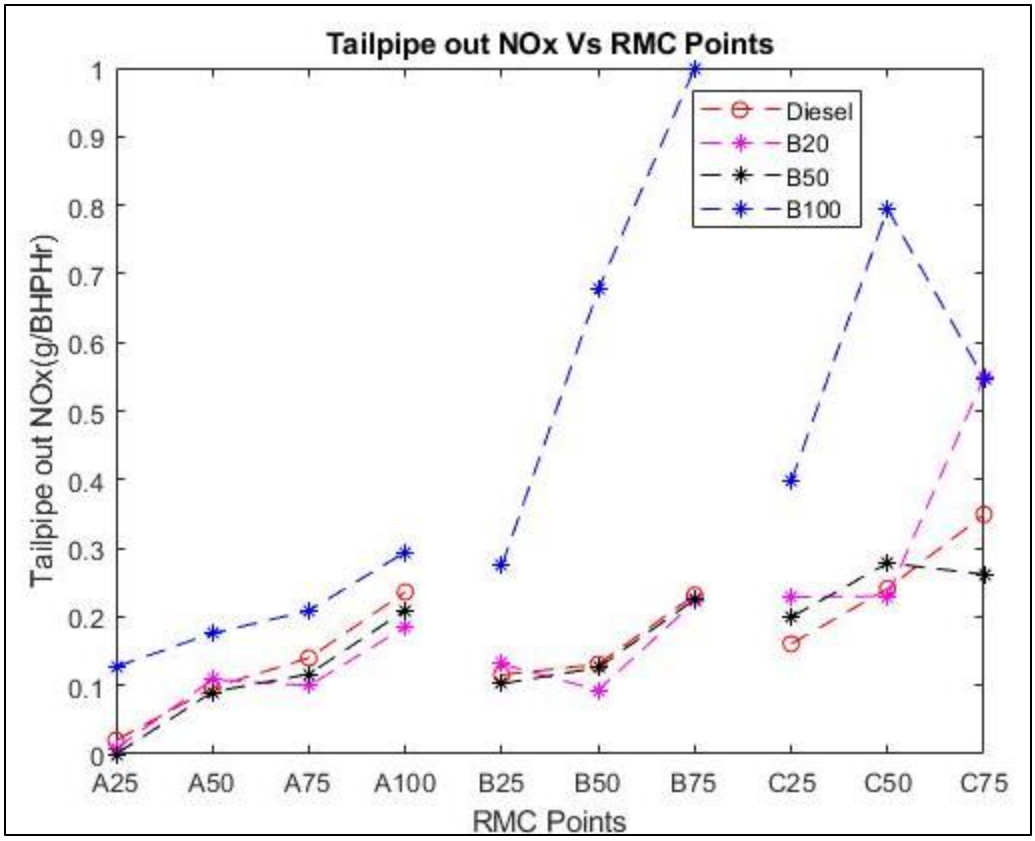

Figure 26: Tailpipe out NOx

As discussed in section 1, it was expected that biodiesel being oxygenated fuel, leading to higher temperatures due to fuel bound oxygen, will have higher exhaust temperatures. However, as biodiesel has lower density and lower heating value, it commanded higher fueling rates and higher exhaust flow, this led to reduced temperatures at engine out. As seen in fig 27 and 28, DOC and SCR inlet temperatures were observed to be reduced with increase in biodiesel blend percent. The most significant reductions observed in B100.

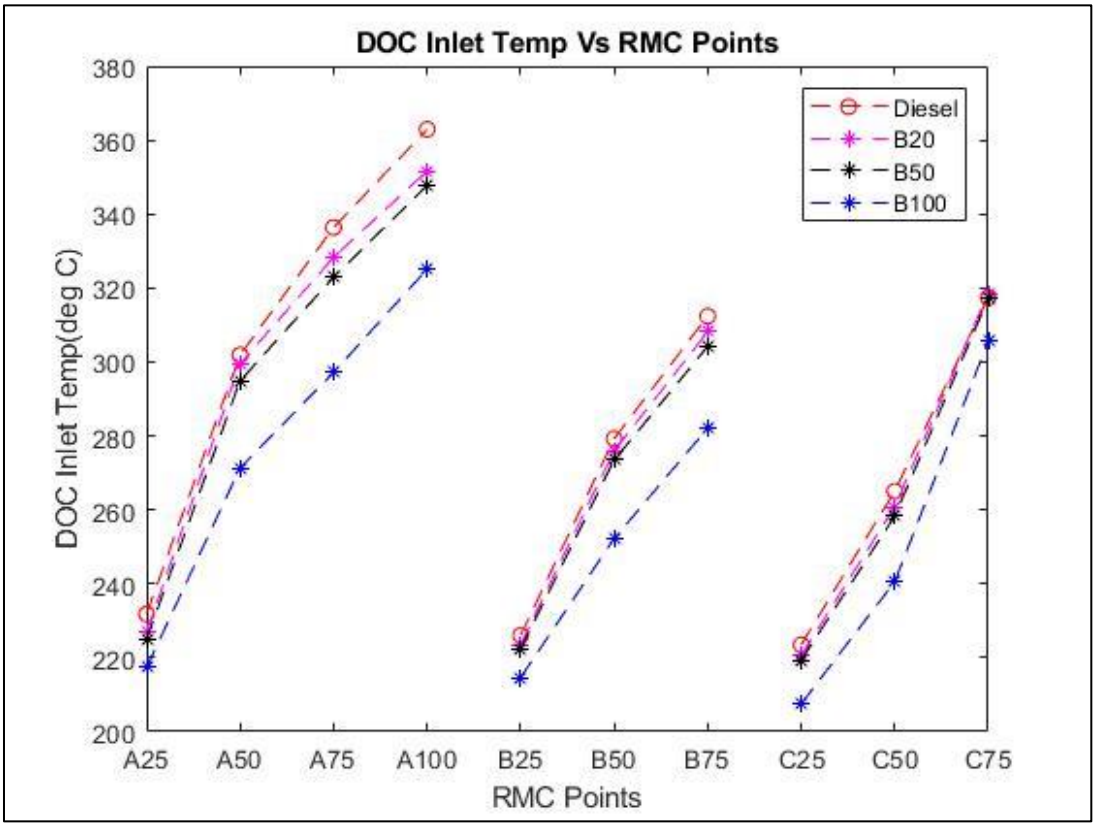

Figure 27: DOC inlet temperature

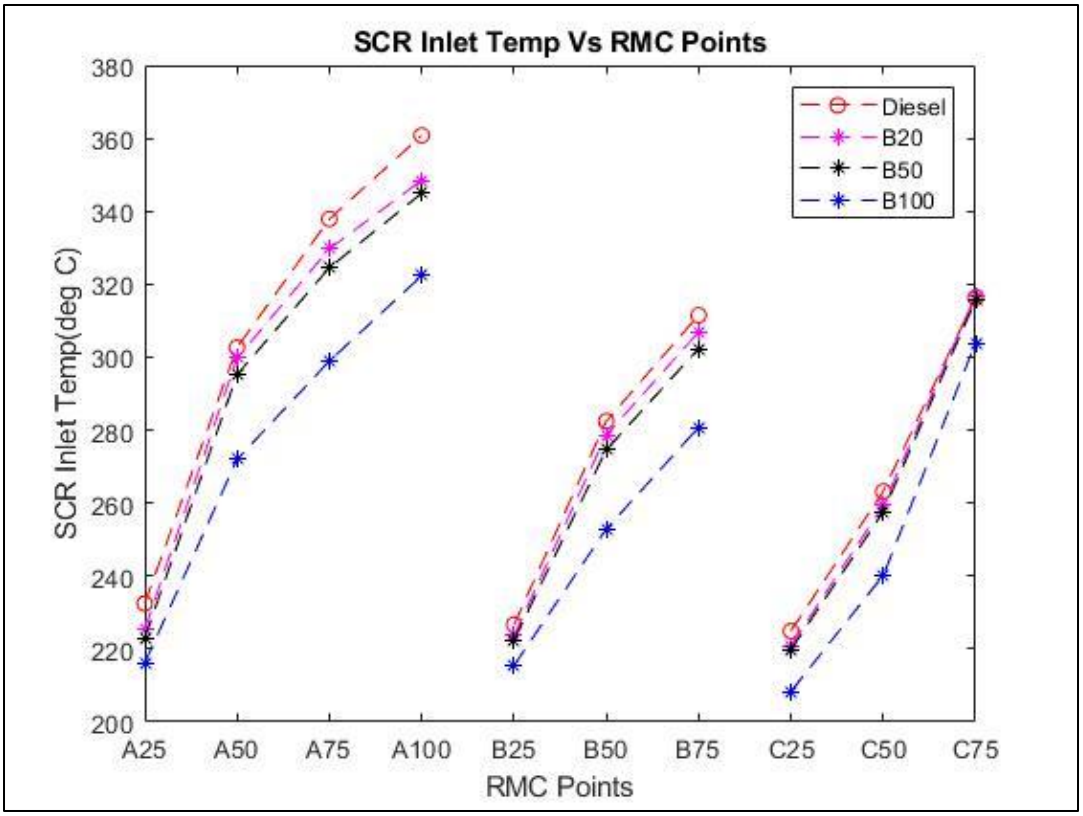

Figure 28: SCR inlet temperature

As biodiesel combustion results in higher amount of engine out NOx, it commanded higher amount of urea to be dosed. This was seen as significantly increased urea injection was observed with increase in biodiesel blend percent (see fig 29).

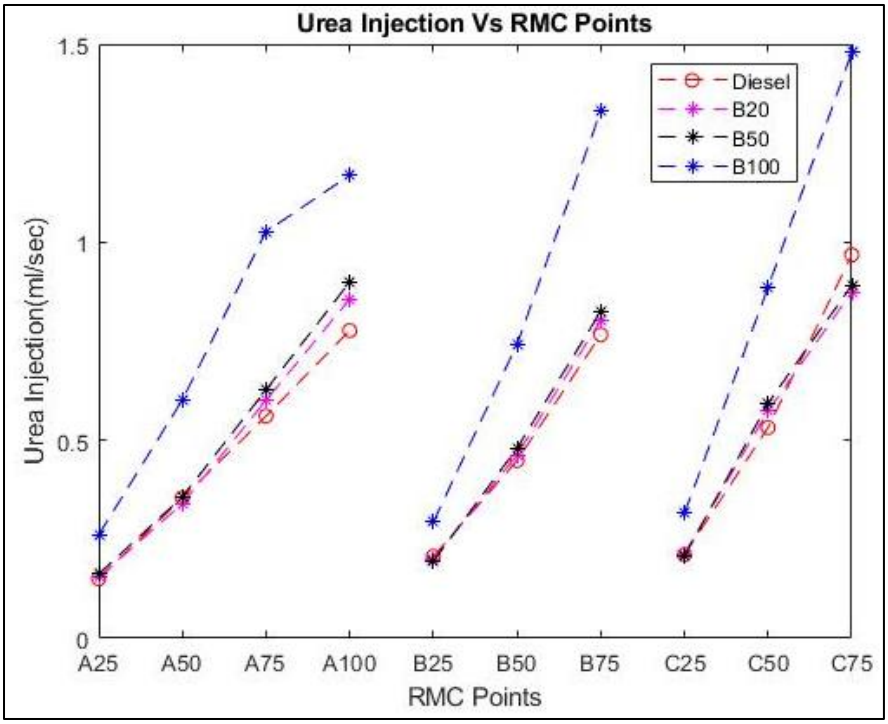

Figure 29: Urea injection rate

As seen in fig. 30, injection timing was observed to be advanced at low loads and retarded for high loads compared to diesel with increase in biodiesel blend percent. Retarded injection timing is expected to assist in lowering NOx by reducing reaction in cylinder [12], however this was not observed here. This could be due to reduced EGR flow observed in this case (fig. 31)

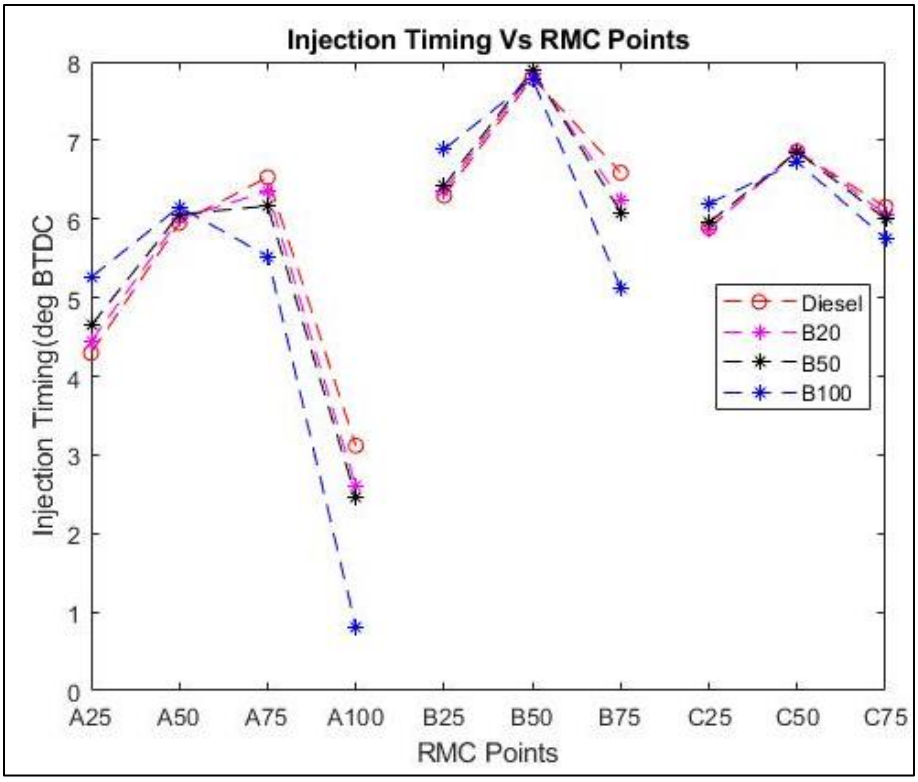

Figure 30: Injection timing

EGR is an effective way to reduce NOx as recirculating the exhaust gas through cylinder again, dilutes the O_2 content which helps reduce NOx formation. As seen in fig.31, in these experiments, EGR fraction was observed to be reduced with increase in percent of biodiesel blends. This in turn resulted in more NOx as seen in fig. 25 and 26 above.

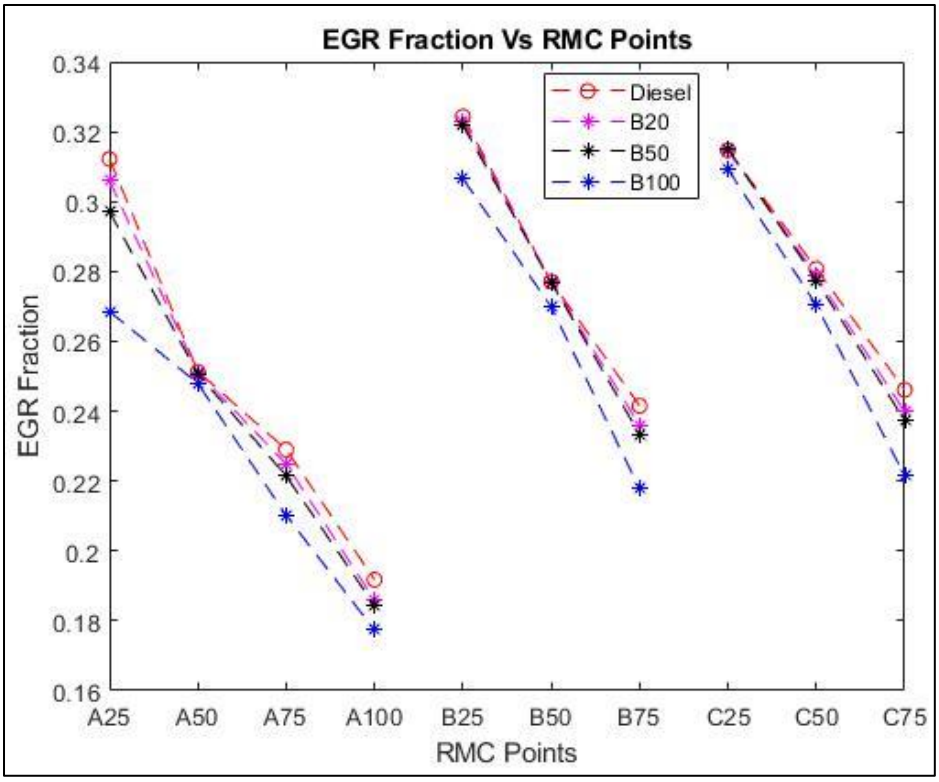

Figure 31: EGR fraction

As discussed above, owing to the lower density of biodiesel, it commanded higher fueling and consequently higher air flow. Thus, fueling rate was observed to be increased with increase in biodiesel blend percent (see fig. 32) and higher exhaust flow rates were observed for increase in percent biodiesel blend (fig. 33).

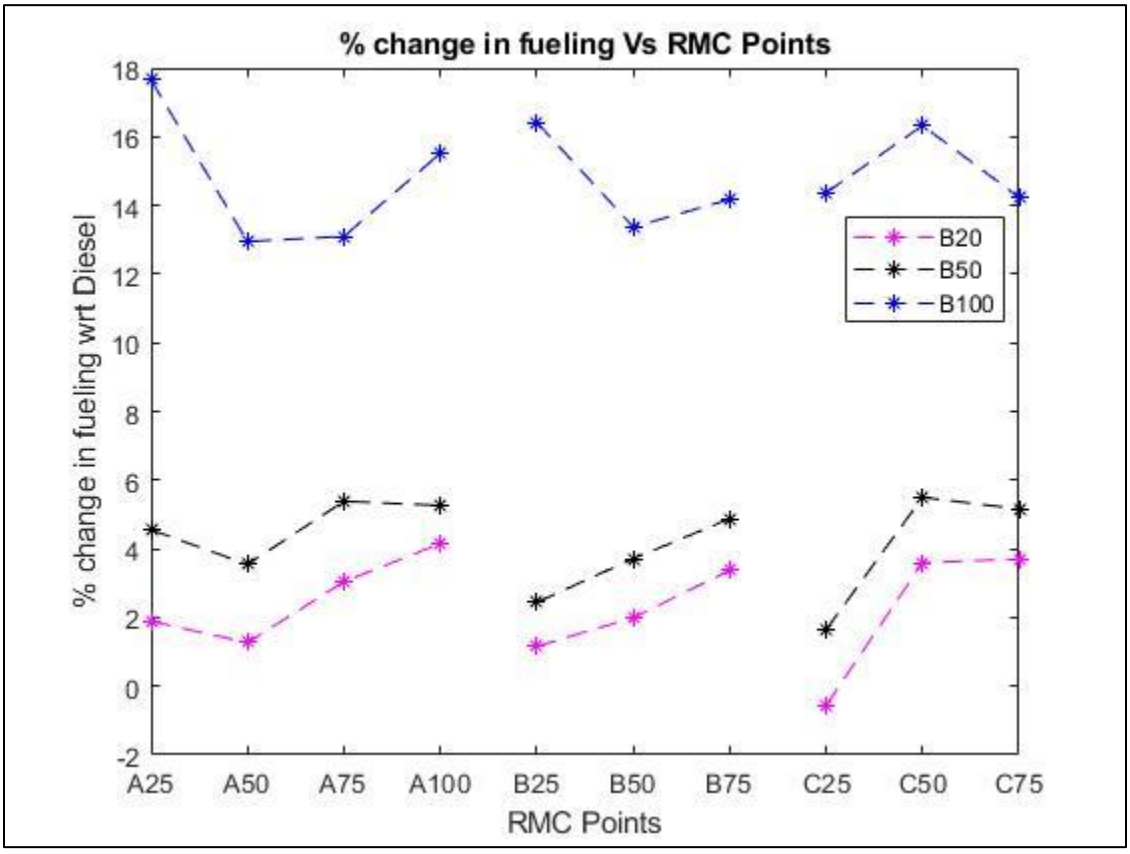

Figure 32: Percent change in fueling

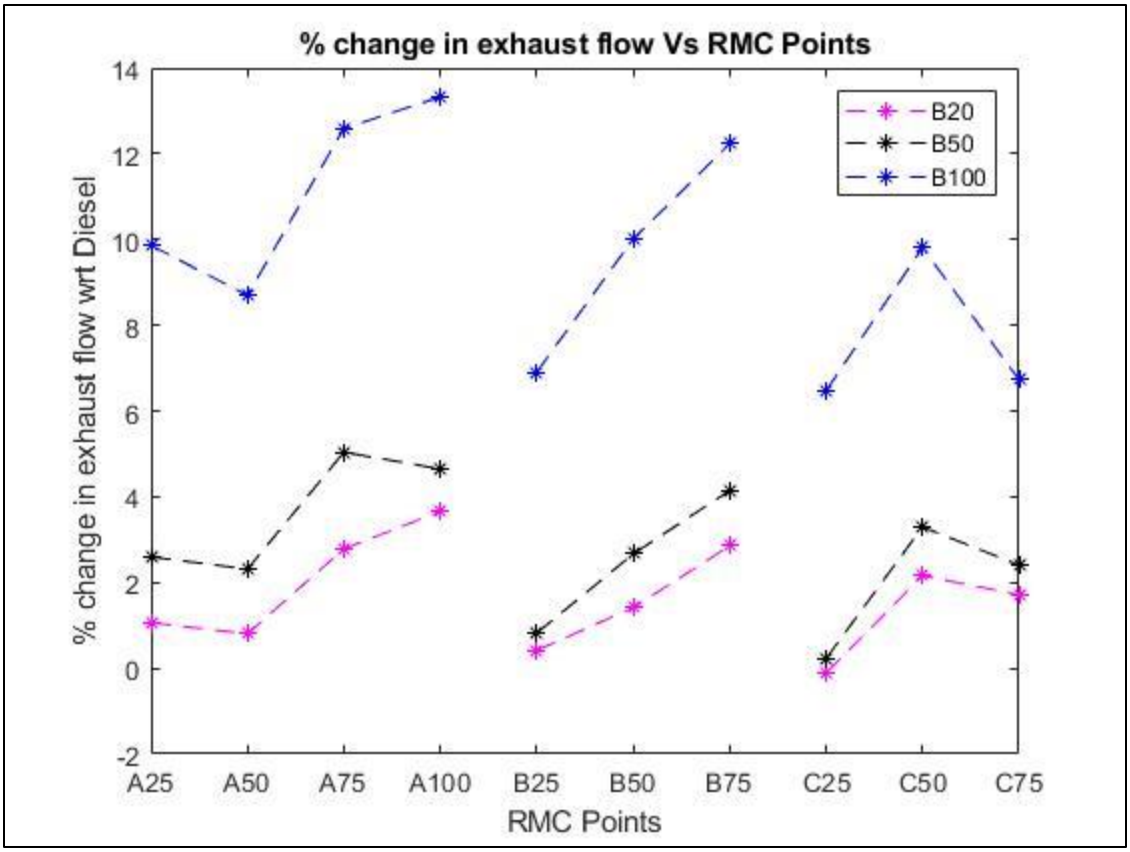

Figure 33: Percent change in exhaust flow rate

5.2.2 Error bars

The data available from the steady state testing was analyzed based on the statistical average values obtained over 5 minutes at 5 Hz frequency of data logging at each steady state point. To understand the range of variation of this data, error bar analysis was performed. Error bars are calculated as ±1 standard deviation away from the mean values.

It was observed that most of the calculated standard deviations are insignificant, except engine out NOx and tailpipe out NOx as shown in plots below.

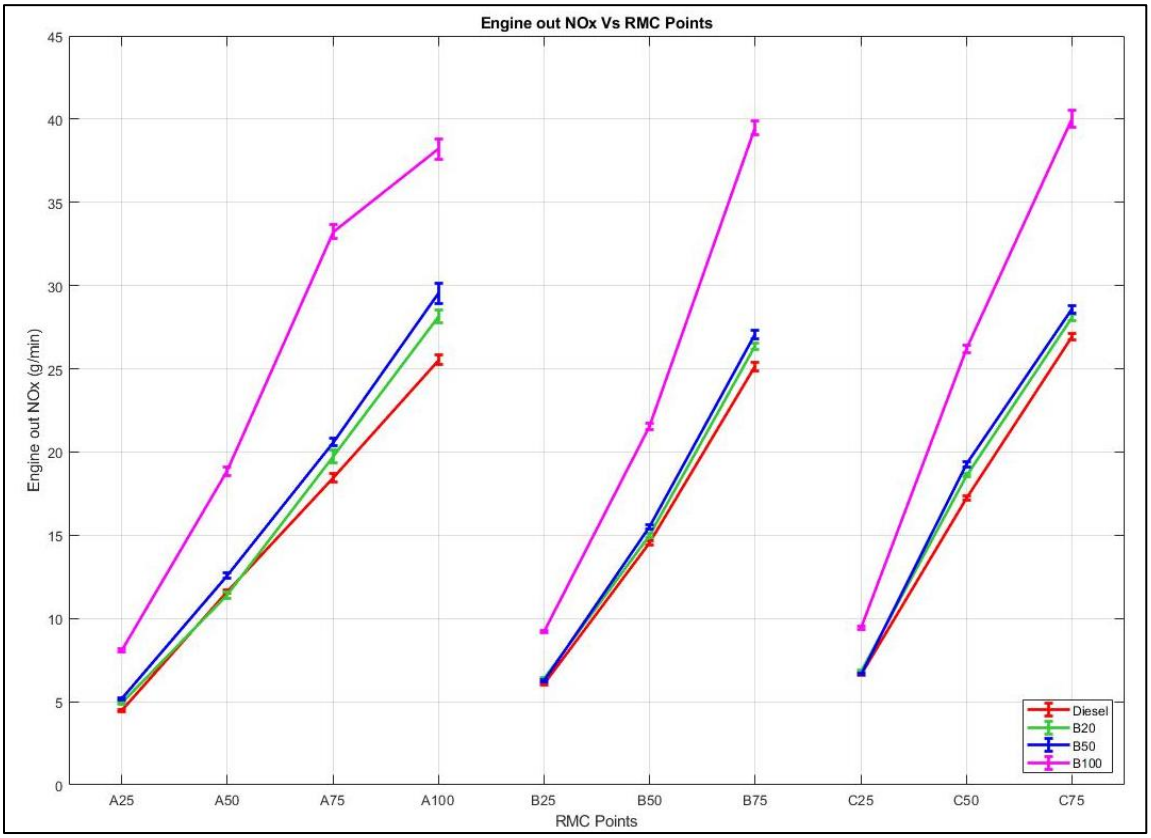

Figure 34: Error bars for engine out NOx

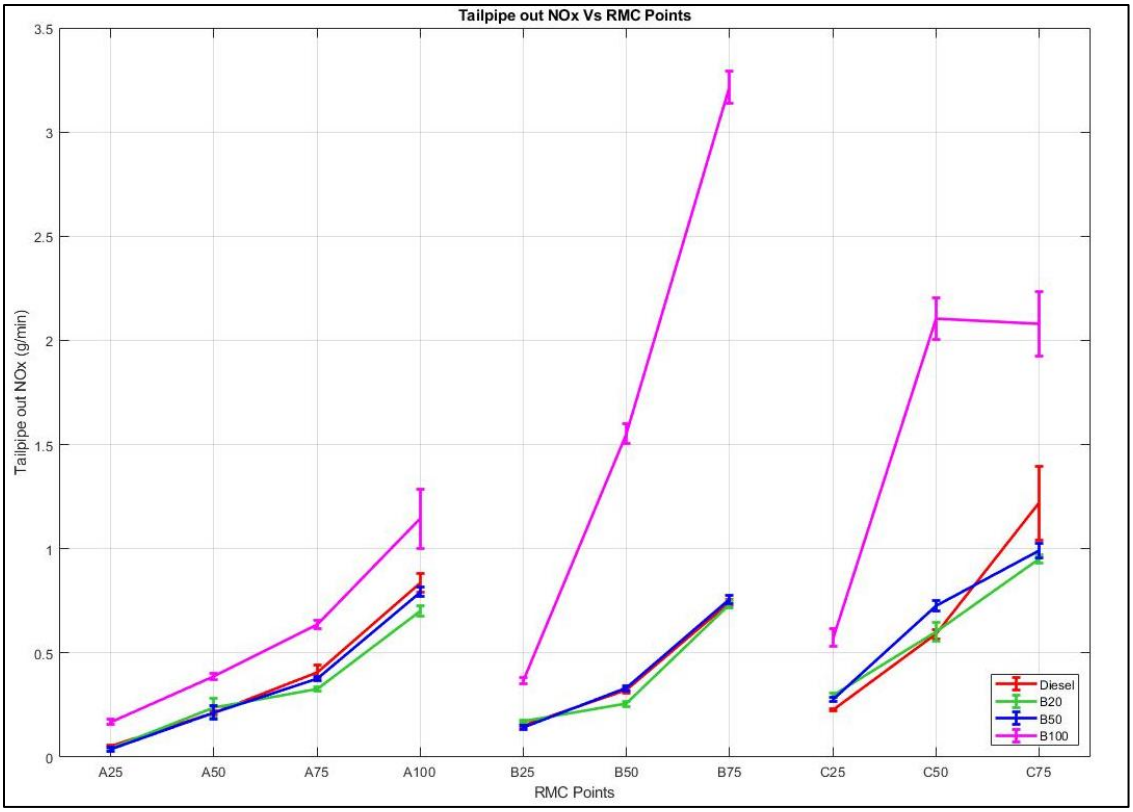

Figure 35: Error bars for tailpipe out NOx

5.2.3 Combustible Oxygen Mass fraction

Combustible oxygen mass fraction is measure of amount of oxygen available for combustion in a fuel molecule. It is defined as below –

$$\frac{Y_{O2,air} * \dot{m},\ air\ +\ Y_{O2,EGR} * \dot{m}, EGR + Y_{O2,fuel} * \dot{m}\ fuel}{Y_{O2,air} + Y_{O2,EGR} + Y_{O2,fuel}}$$

where, Y_{O2} refers to oxygen fraction by mass in intake air, EGR and in fuel and $\dot{m}$ refers to mass flow rates of intake air, EGR and fuel. Mass flow rates were available from the engine ECM and oxygen fraction is used as below

Table 3: Oxygen mass fraction

Parameter	Value
$Y_{O2,\ air}$	0.21
$Y_{O2,\ B100}$	0.109
$Y_{O2,\ Diesel}$	0

For oxygen fraction in EGR ($Y_{O2, EGR}$), engine ECM data for EGR fraction and percent oxygen in exhaust is used for the calculations.

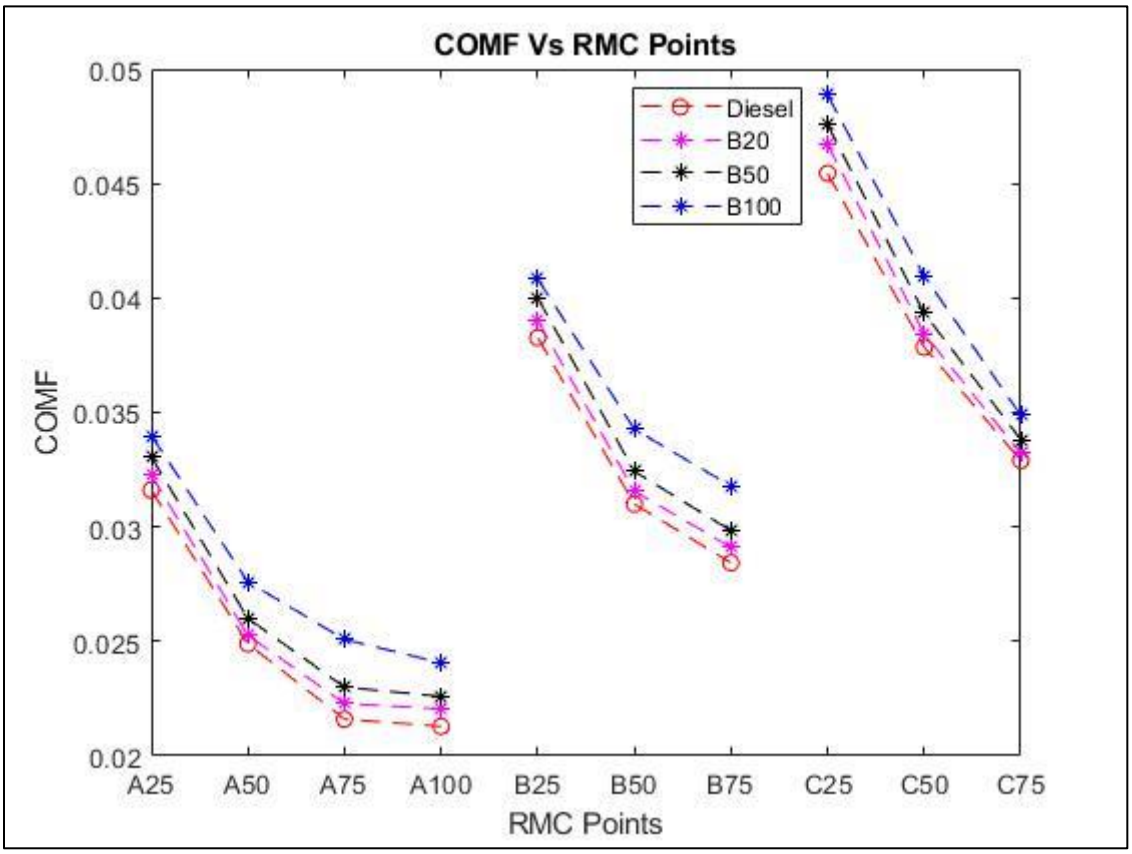

Figure 36: Combustible oxygen mass fraction

It was observed that combustible oxygen mass fraction (COMF) is higher for biodiesel blends as compared with diesel. Referring to NOx plots in previous section (fig 29 and 30), it can be inferred that higher COMF has direct relation with higher NOx.

5.2.4 Density analysis

As previously stated, soy biodiesel is less dense than the conventional diesel (Table 1). We would expect fueling for B20 to be 20% and B50 to be 50% of the way between Diesel and B100, but this was not the case (fig.32 and fig. 37).

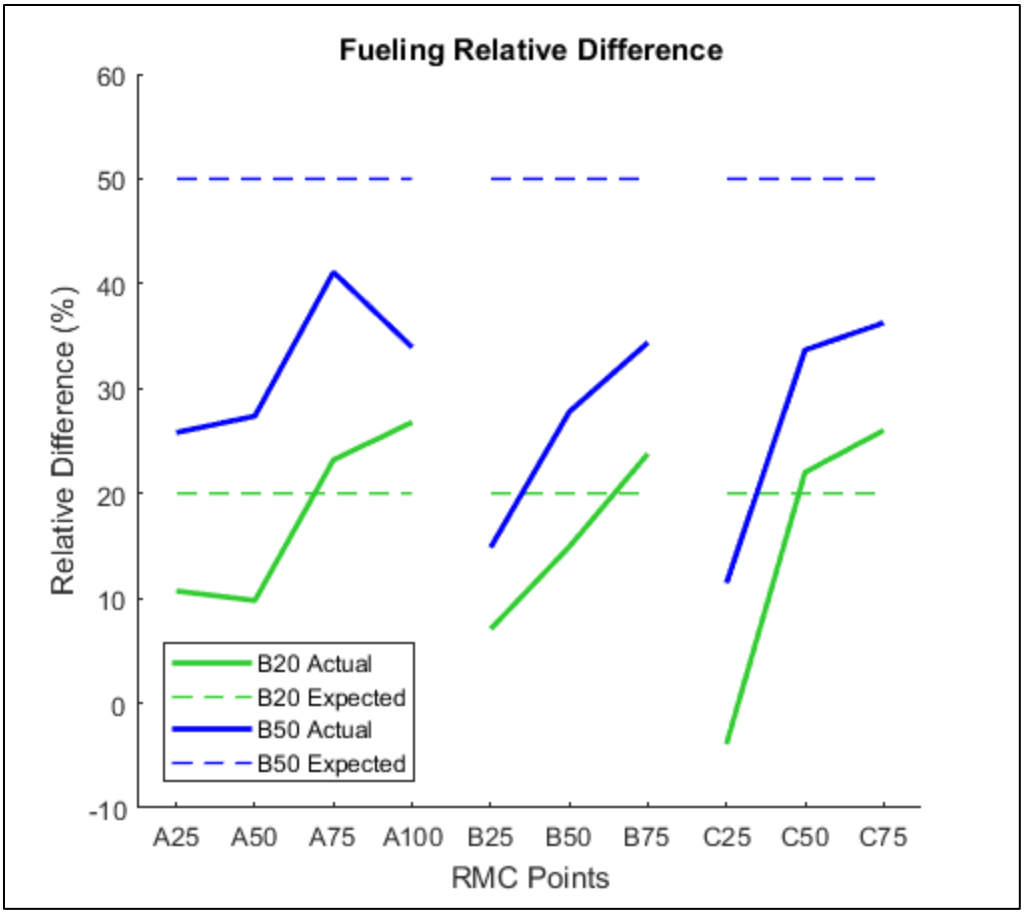

Figure 37: Fueling relative difference

This could be because of the following reasons –

Hypothesis 1: Fuel was not proportioned properly during manufacturing

Hypothesis 2: More diesel is being injected than biodiesel

Hypothesis 3: Diesel separates from biodiesel because of density

Hypothesis 4: Fuel pumps from bottom of bucket (more dense fuel is more likely to get pumped out first)

Based on above, a quick check was performed to weigh known volumes of fuels in a container with known volume and check density of each fuel.

Following Methods were used in the experiments –

1) Herrick lab Shop provided scale – this was a digital scale and had a resolution of 10 grams

2) Fuel bucket load scale – this was an existing weighing scale inside the fuel bucket in engine test bed.

3) Fuel bucket load scale using slightly different method – this was done with altering the moving average of the Simulink model that logs the weight data.

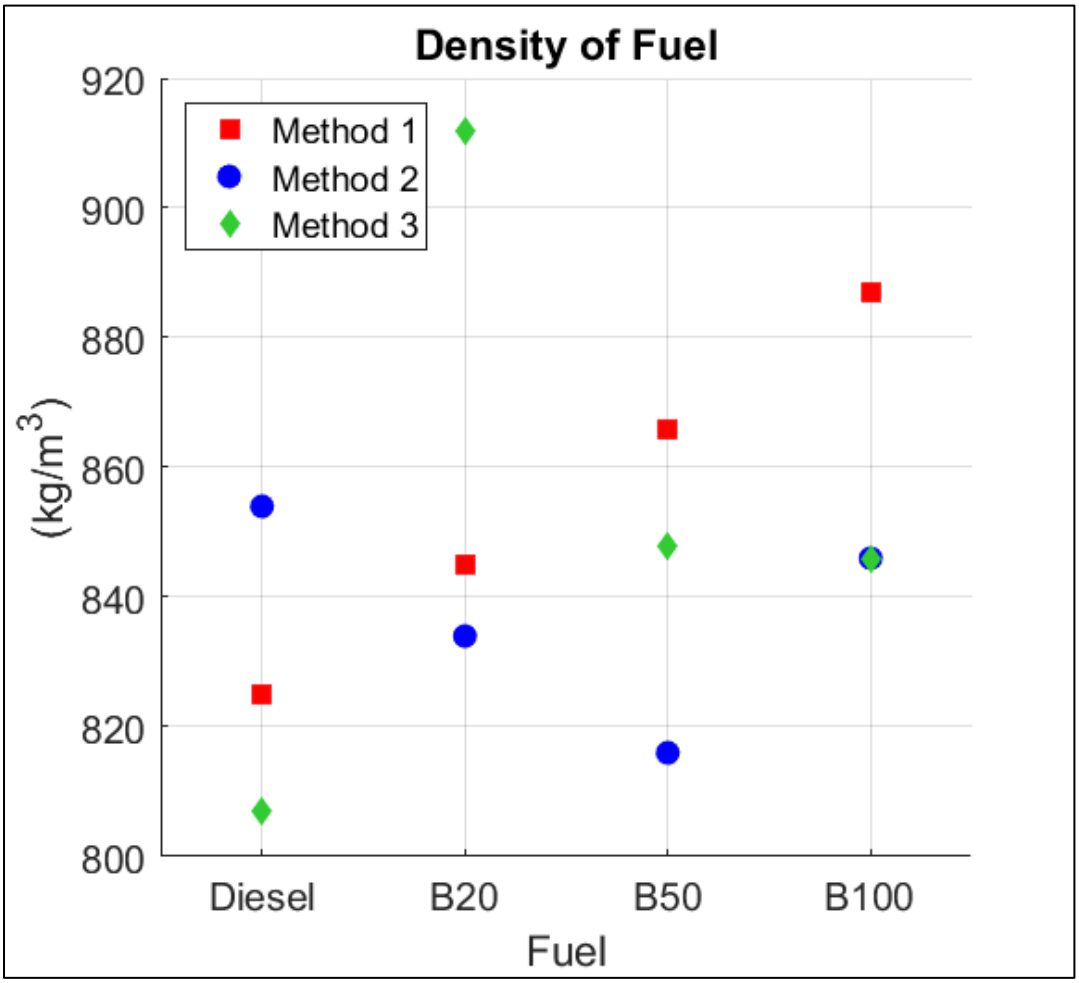

Figure 38: Fuel density

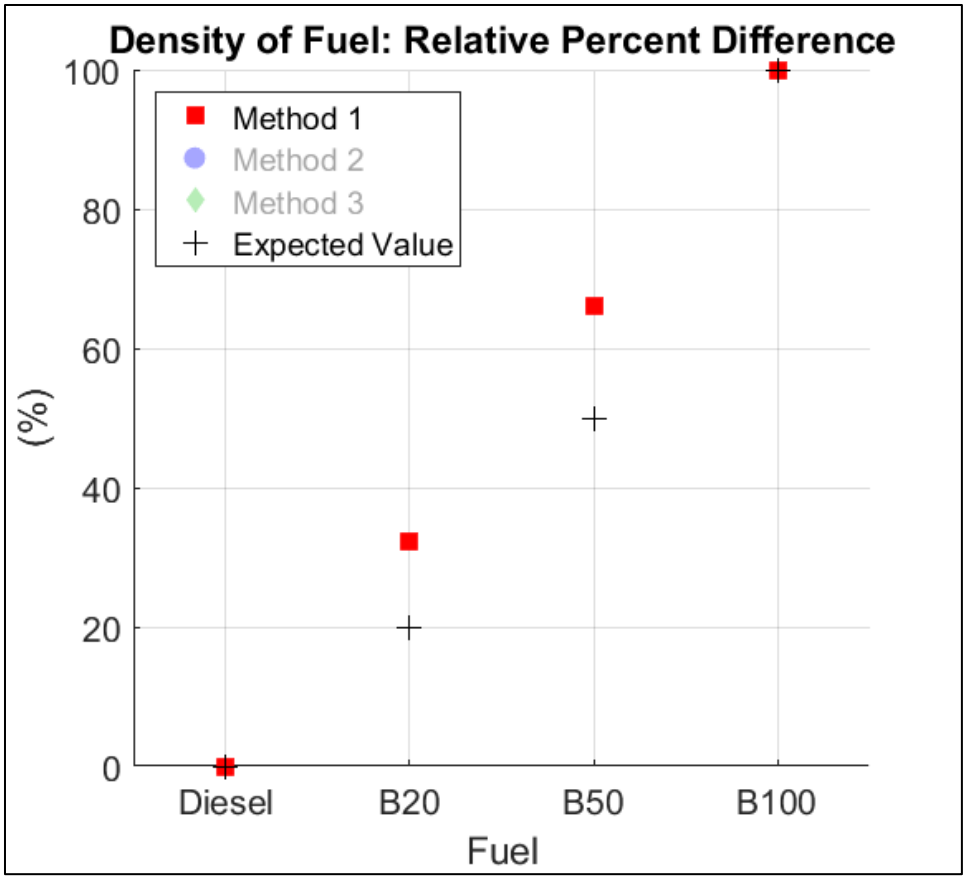

Figure 39: Density of fuel- relative difference

Expected density of diesel is around 828 g/L (refer Table 1) while density of 100% biodiesel B100 is 863 g/L. Thus, it was expected that experimental data would also show that biodiesel is denser.

As can be seen in fig. 39, density reported by Method 1 was low and was most likely due to low measurement of volume (low by about 15 mL ~ .5 oz)

The relative difference calculated by Method 1 is closer expected value but is limited by resolution of scale, however drawing coherent conclusions from method 2 and 3 which used load cell was not possible due to no clear trend. This could be because there was a high chance of manual interference in method 2 and 3 while emptying the fuel bucket after each blend and then re-filling it. This might also change the bucket C.G due to change in bucket orientation in each experiments which will affect the weight reported in Simulink model.

Thus, weights reported by a simple digital weighing scale in Method 1 were more sensible to be used. Biodiesel proportions appear to be accurate given results of Method 1

6. CONCLUSIONS

Natural gas VVA –

The main benefits of IVC modulation are that there is a considerable fuel benefit – 2%-9% reduction in fuel flow rate and there is an increase in efficiency – 1%-3% increase in BTE. Other important benefits include reduction in pumping losses at low loads and increase in open cycle efficiency.

The challenges included validation of the GT power model with engine data as well as including the realistic heat release model to gain more confidence on the closed cycle efficiency calculations, in cylinder pressures and temperatures.

Biodiesel –

In conclusion, it can be said that biodiesel blend B100 produces significantly higher engine out and tailpipe out NOx, it has reduced DOC inlet and SCR inlet temperatures and significantly increased urea injection.

Fuel flow and exhaust flow rates are significantly increased for biodiesel and EGR fractions are reduced. There is no clear trend for injection timing observed, as it was advanced for lower torques and delayed for higher torques. However retarded injection timing could be beneficial for NOx reduction if EGR targets are adjusted.

One of the limitations of the experiments was that it was not possible to run as high torque as with diesel. This is due to lower energy density of biodiesel compared to diesel and due to calibration limits of the stock engine.

6.1 Future scope

Natural gas VVA – There is a scope of modification of the existing GT power model with inputs from test cell data (fuel map data) and rerunning IVC modulation strategies with the calibrated model. As the current model has a constant heat release rate which would change ECR values, re-run with actual heat release rates is needed. Another important parameter that needs to be studied is knock mitigation benefits from the IVC modulation strategy in GT Power. There are few already established knock prediction models and methods which can be implemented in the GT power model. Further, this can also be validated in the experiments run on actual engine in the test cell.

Biodiesel – this research can be further taken into developing engine control strategies for biodiesel. As seen in section 5, there is a scope to work on engine controls to accommodate the biodiesel blends and to modify the fueling rates, after treatment thermal management, urea dosing rates and EGR fractions to name a few. These will further affect NOx values at engine and tailpipe out. Also, it would be good to run the transient and regulatory testing with the biodiesel blends and to study the emission species if they conform to EPA 2024 or beyond.

6.2 Key Takeaways

Below are the key takeaways from these projects:

Natural gas VVA:

Fuel savings – there are fuel saving benefits in terms of reduced fuel flow and reduced brake specific fuel consumption with IVC modulation

Efficiency improvements – open cycle efficiency and brake thermal efficiency improved with IVC modulation

Expected reductions in emissions – reduced in-cylinder temperatures are expected to help in reducing NOx emissions

Biodiesel:

Increased engine out and tailpipe out NOx for biodiesel – with increase in biodiesel blend percentage, engine and tailpipe out NOx was observed to be increased

Need engine calibrations/tuning for accommodating biodiesel blends – to effectively use biodiesel blends with existing diesel engines, it needs to be calibrated and tuned accordingly.

REFERENCES

[1] "https://www.eia.gov/energyexplained/diesel-fuel/diesel-and-the-environment.php."

[2] "https://www.eia.gov/energyexplained/natural-gas/natural-gas-and-the-environment.php#:~:text=Natural%20gas%20is%20a%20relatively%20clean%20burning%20fossil%20fuel&text=About%20117%20pounds%20of%20carbon,MMBtu%20of%20distillate%20fuel%20oil."

[3] "https://farm-energy.extension.org/soybeans-for-biodiesel-production/#:~:text=Soybean%20oil%20is%20currently%20a,which%20acts%20as%20a%20catalyst)."

[4] "https://www.eia.gov/todayinenergy/detail.php?id=39372."

[5] "U.S. Energy Information Administration, Monthly Biodiesel Production Report, and U.S. Department of Agriculture."

[6] G. B. Parvate-Patil, H. Hong, and B. Gordon, "Analysis of Variable Valve Timing Events and Their Effects on Single Cylinder Diesel Engine," Oct. 2004. doi: 10.4271/2004-01-2965.

[7] R. Modiyani *et al.*, "Effect of intake valve closure modulation on effective compression ratio and gas exchange in turbocharged multi-cylinder engines utilizing EGR," *International Journal of Engine Research*, vol. 12, no. 6, pp. 617–631, Dec. 2011, doi: 10.1177/1468087411415180.

[8] A. Garg *et al.*, "Fuel-efficient exhaust thermal management using cylinder throttling via intake valve closing timing modulation," *Proceedings of the Institution of Mechanical Engineers, Part D: Journal of Automobile Engineering*, vol. 230, no. 4, pp. 470–478, Mar. 2016, doi: 10.1177/0954407015586896.

[9] C. Kuruppu, A. Pesiridis, and S. Rajoo, "Investigation of Cylinder Deactivation and Variable Valve Actuation on Gasoline Engine Performance," Apr. 2014. doi: 10.4271/2014-01-1170.

[10] D. B. Snyder, G. H. Adi, C. H. Hall, and G. M. Shaver, "Control-variable-based accommodation of biodiesel blends," *International Journal of Engine Research*, vol. 12, no. 6, Dec. 2011, doi: 10.1177/1468087411415181.

[11] C. M. Hall, G. H. Adi, G. M. Shaver, and B. Tao, “A robust fuel flexible combustion control strategy for biodiesel with variable fatty acid composition during mixing-controlled combustion,” *International Journal of Engine Research*, vol. 15, no. 2, Feb. 2014, doi: 10.1177/1468087412465276.

[12] S. Maroa and F. I. Biodiesel, “Green Energy and Technology.” [Online]. Available: http://www.springer.com/series/8059

[13] “https://www.cumminswestport.com/models/b6.7n.”

[14] D. W. Stanton, “Systematic Development of Highly Efficient and Clean Engines to Meet Future Commercial Vehicle Greenhouse Gas Regulations,” *SAE International Journal of Engines*, vol. 6, no. 3, Sep. 2013, doi: 10.4271/2013-01-2421.

[15] “https://x-engineer.org/automotive-engineering/internal-combustion-engines/performance/mechanical-efficiency-friction-mean-effective-pressure-fmep.”

[16] “https://dieselnet.com/tech/cat_scr.php#:~:text=In%20the%20United%20States%2C%20SCR,hr%20for%20heavy%2Dduty%20engines.”

[17] “https://www.cummins.com/components/aftertreatment/on-highway.”

[18] “https://dieselnet.com/tech/engine_heavy-duty_aftertreatment.php.”